We'd like to thank both the reviewers for taking the time to read our paper submission and give their expert feedback. In the following document we have addressed their remarks and indicated where the specific changes to the document have been made. All line numbers are with regards to the tracked changes document.

Referee: 1

The article submitted by V. Onink and collaborators and entitled Empirical Lagrangian parametrization for wind-driven mixing of buoyant particles at the ocean surface, presents numerical results on the vertical motion of plastic particles induced by wind-driven mixing in a one-dimensional Lagrangian model of the ocean surface. The authors investigate two types of stochastic approaches to mimic the upper-ocean turbulent diffusion, as well as two different profiles of diffusion in the vertical based on published studies. They compare their numerical outputs, mainly the mean concentration profiles for plastic with different rising velocities, with observations from 5 previous studies (4 published, 1 unpublished).

The material presented here is well structured and clear, with the appropriate level of English. It corresponds to an interesting implementation of a Lagrangian transport model for plastic pollution based on models reproducing the properties of turbulence in the upper-ocean, and the authors indeed emphasized that their approach is compatible with more complex OGCM (Ocean Global Circulation Model) approaches.

We would like to thank the reviewer for these kind words.

However, the discussion of the results made by the authors is limited to simple metrics. Furthermore, more efforts could be made in the description of the model implementation (although the code is available at a Zenodo deposit).

In the end, I have the impression that the results are not sufficiently discussed, and below are my main recommendations for the manuscript to be improved, before granting publication.

1. In §2.1, the code used for the study is described with little details. The code Parcel is clearly made for 2D or even 3D studies, but it is not clear to me how it is transformed to solve onedimensional problems, in the vertical. What is the horizontal domain like, what is the rule of transport for the 100,000 particles transported all simultaneously launched at the same depth at the beginning? Much more details are required here. There are no details on the spatial resolution as well.

Parcels is indeed a python package that has been used for 1D, 2D and 3D Lagrangian studies, and we hope that our changes at lines 100 - 105 together with the code documentation at Zenodo give sufficient detail of the model setup. In short, we start with releasing 100,000 particles simultaneously at z=0, and we compute the vertical transport according to equations 3

- 7 depending on the scenario. We set the horizontal velocities to zero (thereby reducing the model to a 1D setup), and hence don't prescribe any horizontal domain. Finally, we calculate the K_z fields with a vertical spatial resolution of 0.1 m, with the K_z value at the particle position being linearly interpolated from these values.

2. The comparison of the model outputs with the observations is made by using a single metrics, the root mean square error between mean profiles and a "normalized " field measurements. First a clear definition of the expression used is required although it might seems obvious, to avoid any confusion. Furthermore, it seems a bit too simplistic. Since the many profiles are not all with the same uncertainty, or the same flow conditions, some higher level of analysis could be made for the observations. Similarly, the temporal "steady" profile is not the only quantities to extract and variance at least would be of interest. Furthermore, the global comparison of a profile with observations by averaging with depth is possibly putting a lot of importance on strong errors at large concentrations although the overall profile could be 'on appearance' correct.

We have added a definition of the RMSE at line 202 to clearly define the metric we use throughout the analysis. We acknowledge that the RMSE is not a perfect metric, but we struggled to find a better alternative. We looked at the correlation between the field data and model data (see the figure below), but we did not consider this a very informative metric because modeled decreasing concentrations with depth already provides a very high correlation; so the RMSE metric is much more stringent. Hence, we don't necessarily see the added value of including this metric.

We generally only have field concentrations, the wind and MLD (either precalculated or we could calculate it from provided CTD data) conditions at the time of sampling. Ideally we'd have wind speeds, MLD and langmuir mixing data for the hours leading up to the actual sampling to try and replicate the variability in ocean conditions, but as we state in lines 317 - 319, we are limited in the analysis we can do due to lacking such data, and we highlight in lines 325 - 327 and 336 - 338 that collecting more detailed information of sampled microplastics and the oceanographic conditions at the time of sampling would help further develop models such as ours. Nevertheless, we have expanded our analysis. We estimate the variability in the field measurements by binning the normalized field concentrations into 0.5 m bins and calculating the standard deviations over the binned data points for all wind conditions. While a large part of this variability is likely driven by time-varying ocean conditions or by e.g. different Langmuir mixing conditions under similar wind speed conditions (as stated in lines 315 - 323), it does provide a more robust estimate of the variability than solely plotting all field points. Due to the static wind and MLD conditions, the model variability is significantly smaller, but we do visualize this variability by shading around each profile, where the shading indicates the standard deviation at each depth level calculated over the final hour of each model simulation (Figures 2, 3, 5). We also better illustrate the time evolution of each profile in supplementary figure C1, which shows how quickly the model reaches an equilibrium assuming static wind and MLD conditions.

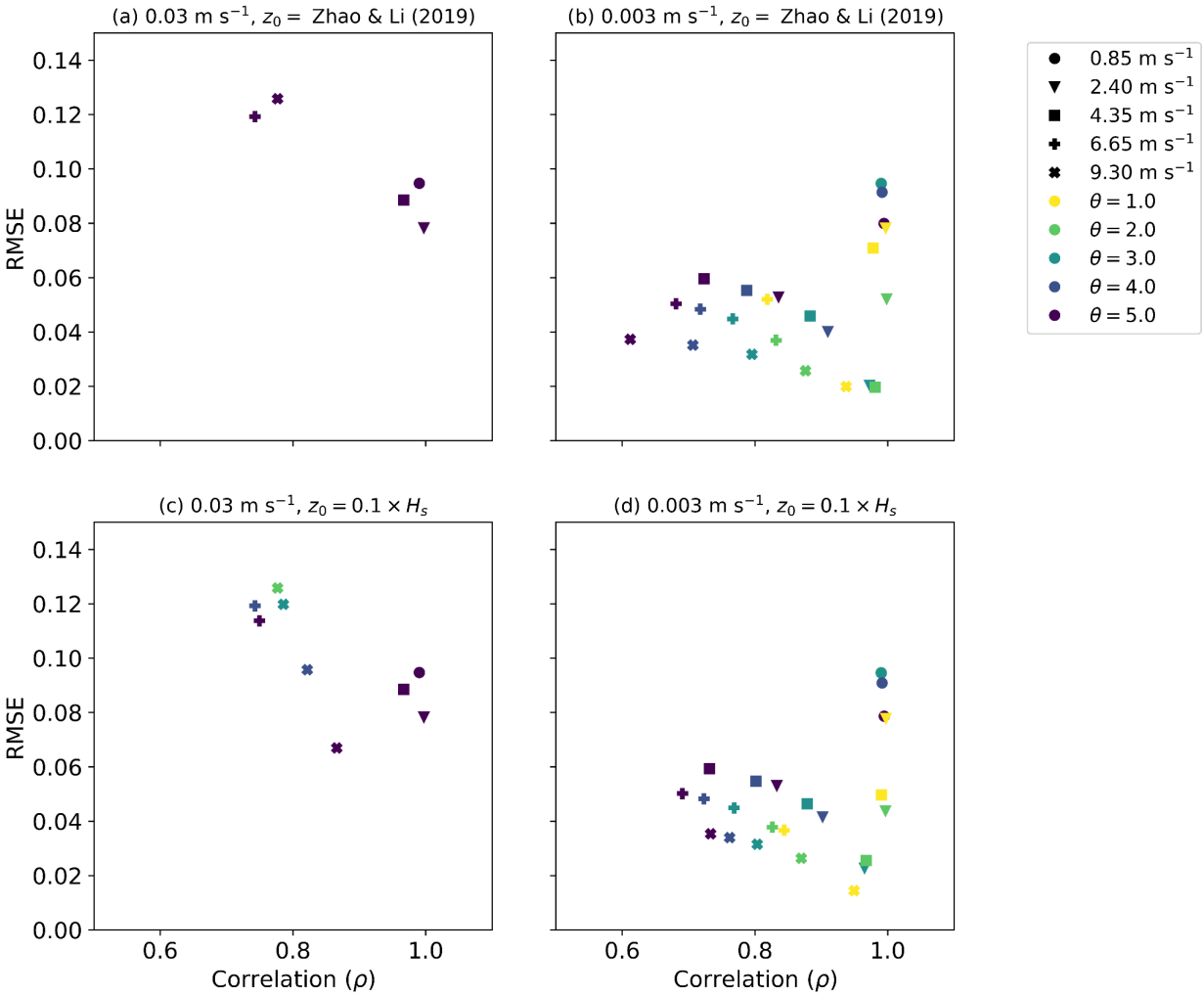

3. The case of the fastest rising particles is disappointing. The difficulties in terms of temporal resolution should be discussed in more depth, with some comments made on time intervals for fast objects related to the vertical resolution of the models too (0.03*30 1m ... to compare with vertical resolution). Furthermore, for the numerics to be relevant, some stronger recommendations in the conclusion should be made. To my mind, the modeling of such particles is not possible for current OGCM models unless a specific choice of temporal / spatial resolution is made, but I am not sure it is the correct interpretation to have here

We thank the reviewer for this insight. Indeed, the high buoyancy particles show strong sensitivity to the integration timestep with SWB diffusion, and we highlight this in the conclusions at lines 345 - 346: “The parametrizations generally perform well for timesteps of $\Delta t = 30$ seconds, but for high buoyancy particles users need to take care to use sufficiently short timesteps, especially with SWB diffusion”. We also have expanded the discussion of the

influence that the boundary condition has on this integration timestep dependence in lines 270 - 271: "However, for $\Delta t = 30$ seconds the depth of mixing is now overestimated compared to smaller Δt values (Fig. F2), as with $\Delta t = 30$ seconds and $w_r = 0.03$ m s^{-1} the particle would be reflected up to 0.9 m below the ocean surface solely due to the model numerics. " In the case of the KPP diffusion this sensitivity doesn't appear to be as big an issue, as the near-surface K_z are so small that even with small timesteps, the particle buoyancy dominates any mixing. As such, we feel that generally such high-buoyancy particles can be modelled within current OGCM models, but at least with these mixing parametrizations it appears such particles largely remain at the ocean surface, except in cases of especially strong mixing. As we state in line 274 - 276, it depends on the model application whether the error of ≈ 1m in the particle depths is acceptable, and whether shorter timesteps are computationally feasible: "Depending on the model application and setup, the error in the concentration profile depth (≈ 1 m for high buoyancy particles) might be acceptable. Otherwise, the error can be reduced by using a smaller integration timestep where that is computationally feasible."

Other comments

Here is a list of other points of lesser importance.

- l.78. What is the value of alpha for δt larger than TL (should be 0 I guess) ?

We have updated line 80 to state that we calculate alpha assuming dt <= TL. If dt were to be longer than TL, then the integration timestep would be too large to capture all relevant turbulent fluctuations, and a smaller timestep would be necessary.

- l.102. The study is based on three sets of particles having different 'rise' velocities. It would be useful to discuss the values in comparison with the turbulent properties of flow (variance of w 0 for instance).

We have added table A1 to show ratio of the rise velocity to the peak w' value for varying diffusion types and wind conditions, where w' is calculated with equation 3 for dt=30 seconds. We then briefly discuss this comparison of w_r and w' in lines 111 - 114.

- l.140. The introduction of θ is too succinct to be understood, more details like 'θ is a Langmuir circulation enhancement factor that one can adjust between XX and YY, we choose θ = 1 which corresponds to ..."

Due to the feedback from reviewer 2, we have a much more extensive analysis on the influence of the Langmuir circulation enhancement factor θ. As explained in lines 156 - 159, the presence of Langmuir circulation can significantly increase the amount of turbulent mixing within the mixed layer, and we investigate the influence of this by settings $\theta \in [1.0, 2.0, 3.0, 4.0, 5.0]$. As shown in figure 3, this can significantly increase the depth to which mixing occurs, and is an important process to consider when modelling vertical transport of buoyant microplastic (lines 226 - 241).

- p5-6. No reference in the text to Figure 1 for KPP profiles.

Fixed, with reference to the figure at line 154.

- p7. Table 1 introduces unpublished data which is almost invisible in the corresponding figures, and it represents a small number of profiles with little representation. Maybe it is not worth including them that way.

The vast majority of data points indeed originate from Kooi et al. (2016), but all these samples were collected within 5m of the ocean surface. Therefore, while smaller in number, the other profiles give us at least some insight of the vertical concentration profile for depths below 5m.

- l.177. Typo 'w10' instead of 'u10' ?

Indeed a typo, and now fixed.

- l.186. (and at other lines too) The use of greater downward mixing is unclear. Discuss it in terms of depth, or larger number of particles at some depths, etc.

Greater downward mixing can indeed be interpreted in various ways, and we've changed throughout the results and discussion to refer to deeper mixing, by which we mean that a greater number of particles is mixed deeper beneath the ocean surface.

- l.195. 'With both KPP and SWB diffusion, M-1 models show increased leads to increased downward mixing of particles with increasing'. I am not sure I get this sentence clearly.

The intended comment was that relative to M-0 models, using an M-1 results in more particles getting mixed deeper below the ocean surface, but the phrasing here did not communicate this clearly. We've rephrased this at line 243 to read "With both KPP and SWB diffusion, M-1 models show deeper mixing of particles as $\alpha \rightarrow 1$ (Fig. 5)."

- l.233-235. The comment suggest that more plastic sampling in depth is needed, which is true, but I think they should also emphasize on the estimates of a proper diffusion model too (or of the eddy viscosity) !

Indeed, we would benefit both from more field sampling of both plastics at depths and further measurements of near-surface mixing to validate mixing/eddy viscosity models. We now added to line 325 - 327 to emphasize this: "At the same time, we would encourage conducting more ocean field measurements of near-surface vertical eddy diffusion coefficient and/or eddy viscosity profiles, as this will allow further validation of the K_z profiles predicted by the KPP and SWB theory with actual ocean near-surface mixing measurements."

- l.238. About the consistency of models. I understand the point by at the same time, why should it be consistent with other tracers if the model is inadequate? Plastics can

also be a good indicator of a better diffusion model to be implemented, because it has a different nature (buoyancy, size, passive, etc). The reverse is of similar interest (test other model for tracers).

That is a good point, and by comparing the modelled vertical concentration profiles with the field data, we show that Langmuir circulation mixing is likely a very important mixing process that needs to be accounted for when using KPP theory. Based on the new results with accounting for Langmuir mixing, we have rewritten this section now at lines 296 - 308 to read: "With regards to necessary data to calculate the diffusion profiles, the SWB approach has the benefit that it only requires surface wind stress data, while KPP diffusion additionally requires MLD data. Furthermore, our results indicate that accounting for LC-driven turbulent mixing improves KPP diffusion model performance, but determining which Θ value to use is not trivial. McWilliams & Sullivan (2000) demonstrated that Θ is inversely proportional to the Langmuir number La, which is defined as $La = \sqrt{u_{*w}/U_S}$ with U_S as the surface Stokes drift. The Langmuir number can conceivably be calculated using OGCM data, but the details of such an implementation will be left for future work with 3D Lagrangian models. Furthermore, KPP diffusion has the advantage that it has been widely used and validated in various model setups (Boufadel et al., 2020; McWilliams & Sullivan, 2000; Large et al. 1994), while such extensive validation has not yet occured for SWB diffusion. Finally, the influence of wind forcing on turbulence is generally assumed to be limited to the surface mixed layer (Chamecki et al., 2019), while with the SWB profile wind-generated turbulence can extend below the MLD. To represent sub-MLD mixing, either a constant K_z value or other K_z profiles could be used, such as the K_z estimates for internal tide mixing as proposed by (de Lavergne et al., 2020)." We then discuss how the results with comparing the modelled vertical concentration with the microplastic measurements allows indirect validation of the KPP and SWB mixing estimates in lines 329 - 338: "The parameterizations have been validated for high/medium rise velocities, and at least for KPP diffusion with Θ>1.0, the concentration profiles resemble those calculated from field observations. This provides confidence in the turbulence estimates from the KPP approach, and as these are independent of the type of particle that might be present, this would suggest the KPP approach can also be applied to neutral or negatively buoyant particles. However, as model verification was only possible for microplastic particulates with rise velocities approximately between 0.03 - 0.003 m s^{-1}, we would advise additional model verification for other particle types where the necessary field data is available. In the case of SWB diffusion, turbulent mixing seems underestimated when further from the ocean surface, and we would advise more validation with field observations before applying this diffusion approach to other particle types."

- l.246-247. One reference is missing for microplastic properties (Kooi. et al,... -¿ Poulain et al. 2018.

We have added references to Kooi et al. (2016) and Kukulka et al. (2012) at line 314, as these are the two studies we use field data from to validate our results that discussed how such vertical concentration profiles arise.

Referee: 2

The manuscript describes the vertical mixing of buoyant particles at the ocean surface, with comparisons made to microplastics field data. The model compares two different eddy diffusivity models, along with two types of Markov modelling (a random walk (M-0) and a higher order random walk which includes an autocorrelation timescale (M-1)).

The simulations do not represent a substantial contribution to modelling science.

We politely disagree with the reviewer and believe that our work is a substantial contribution to modelling science. We address the specific concerns about the diffusion approaches below, but in general there is a need for a near-surface wind mixing parametrization that can be applied to large-scale modelling efforts with OGCM data, and our work provides such a parametrization along with extensively documented model code that can be used as a basis for applying our parametrization to any given (Lagrangian) model setup. OGCM output, especially in the form of reanalysis products, generally does not provide turbulence fields as output, most likely for storage considerations. This severely hinders any 3D modelling studies of buoyant particles such as microplastics, as turbulent mixing is one of the main processes driving the form and depth of vertical concentration profiles; in this manuscript we provide an empirical workaround for this limitation. The reviewer has a number of concerns regarding the mixing/eddy viscosity models that we address below. These comments helped us to further develop our models, and this has resulted in relatively simple and computationally cheap parametrizations of near-surface mixing that capture the main features of vertical mixing, which we see as a substantial contribution to geoscientific model development.

One concern in this manuscript is the usage, discussion, and validation of the eddy viscosity models. The text describes two vertical diffusion models:

The first uses both the well-established Kukulka et al. (2012) for the near surface and extrapolates below using Poulain (2020). Poulain (2020) is a thesis and therefore the results therein have yet to be peer-reviewed. The Poulain (2020) experiment is described as a tank with a vertically oscillating grid. However, it is not clear in the text whether this model has been verified with respect to ocean surface mixing. Using more well-established near surface model would improve the model.

The near-surface parametrization from Kukulka et al. (2012) is indeed widely used to correct surface measurements of microplastic concentrations for vertical mixing, but Kukulka et al. (2012) itself emphasizes that the parametrization is only valid for depths up to approximately 1.5 times the significant wave height. As we now further highlight in lines 136 - 140, oscillating grid experiments have been widely used to study near surface turbulence, and have been shown to reproduce turbulence decay for velocities and dissipation rates that agree with measurements within the ocean surface mixed layer. Poulain (2020) is indeed a thesis, but the OGT experiments described within have been submitted for peer review, which at the time of writing is not finished yet. As such, we cited the thesis for the time being, and will update this to the peer-reviewed

article once it becomes available. However, we have been in contact with the lead author of the study, Dr. Marie Poulain-Zarcos, and she has confirmed that the eddy viscosity profile applied in our work has not changed during the peer-review process.

While direct validation of the eddy-viscosity model with ocean surface mixing has yet to occur, it does agree in general terms with Kukulka et al. (2012) in predicting constant mixing near the surface (within one significant wave height of the surface). The underlying theoretical reasoning behind the parametrization differs from KPP diffusion, and we think this provides an interesting contrasting approach for modelling near-surface mixing. Furthermore, our work provides an albeit indirect validation of the SWB diffusion approach, which seems to underestimate the total mixing throughout the mixed layer as we state in lines 336 - 338: "In the case of SWB diffusion, turbulent mixing seems underestimated when further from the ocean surface, and we would advise more validation with field observations before applying this diffusion approach to other particle types."

The second uses KPP. KPP is a bulk boundary layer model which goes to zero at the free surface. This means that all positively buoyant particles at the free surface would stay at the free surface, regardless of the wind conditions. The text mention this, but does not elaborate. Under this scenario, are their equilibrium profiles initial condition dependent? I would expect after long times, all the particles should stay at the surface, and therefore I'm unsure why simulations are needed when the final state is pre-determined.

We have rewritten lines 153 - 154 to clarify that the K_z value at the surface in our formulation of KPP diffusion is not exactly zero: "As such, K_z rises from a small non-zero value at z=0 to a maxima at z = 1 / 3 MLD, before dropping to K_z=K_B for z ≤MLD (Fig. 1)." Furthermore, we have changed the x-axis in Figure 1 to a log axis, such that it is clear that while the near-surface K_z is very small, it is not equal to zero. The reason for this is that we use a KPP formulation from Boufadel et al. (2020), which introduces a roughness scale of turbulence z_0, which can represent the surface roughness due to surface waves:

$$K_z = \left(\frac{\kappa u_{*w}}{\phi}\theta\right)(|z| + z_0)\left(1 - \frac{|z|}{MLD}\right) + K_B$$

As such, even when z = 0, K_z > 0, and particles can get mixed down below the surface if the turbulence at z=0 is strong enough to overcome the rise velocity. For example, this can be seen in figure 2 for all particle types. In addition, in figure C1 we plot the time evolution of the medium buoyancy particles, which shows that for both SWB and KPP diffusion, the particles form an equilibrium vertical concentration profile due to the balance in buoyancy and turbulent mixing, where at a given time a significant number of particles are below the ocean surface. In changing ocean conditions, such a steady profile might not always emerge because during the time it can take to reach a steady profile (approximately 1- 2 hours according to our model results), the oceanographic conditions can change. However, this constant cycling of particles between different depths can for example affect the horizontal transport as the zonal and meridional ocean currents have been shown to vary with depth (for example, see Tsiaras et al., 2021). As

such, modelling the vertical mixing of buoyant particles is important to model the long-term fate of such particles, demonstrating how a parametrization such as ours can provide a substantial contribution to geoscientific model development.

Tsiaras, Kostas, et al. "Modeling the Pathways and Accumulation Patterns of Micro-and Macro-Plastics in the Mediterranean." *Frontiers in Marine Science* (2021): 1389.

Boufadel, Michel, et al. "Transport of oil droplets in the upper ocean: impact of the eddy diffusivity." *Journal of Geophysical Research: Oceans* 125.2 (2020): e2019JC015727.

The text then compares their simulation results to the observations, and they do not match. In fact, the simulations underpredict the vertical mixing of the microplastics. This is unsurprising, and has been previously demonstrated in the literature, where it has been noted that to fully account for proper vertical mixing of microplastics, one needs to include the effects of breaking waves and Langmuir turbulence (see e.g. Kukulka & Brunner 2015).

While the modelled vertical concentration profiles do show the decrease in concentration with depth as in the field observations, the M-0 models with both KPP and SWB diffusion seem to underpredict the depth to which particles are mixed. In our original approach, we followed Boufadel et al. (2020) in assuming that the influence of Langmuir circulation (LC) driven turbulence was negligible, which in equation 11 for the KPP K_z profile corresponds to setting the Langmuir circulation enhancement factor $\theta = 1.0$. However, as the reviewer notes, studies such as Kukulka & Brunner (2015) and Brunner et al. (2015) have shown that LC-driven turbulence is necessary to properly account for the vertical mixing of microplastics, so we tested the influence θ has on the mixing of our buoyant particles. According to McWilliams & Sullivan (2000), LC-driven turbulence can increase mixing by $\theta = 3\ -4$, so we considered $\theta \in [1.0, 2.0, 3.0, 4.0, 5.0]$ as outlined on lines 156 - 159. As we now show in Figure 3, $\theta > 1.0$ increases the depth to which particles are mixed, and generally increases the agreement between the field observations and the modelled concentration profiles. We acknowledge on lines 299 - 303 that selecting the correct θ value for a simulation is not trivial, as McWilliams and Sullivan (2000) show that this is inversely proportional to the Langmuir number, which in turn can vary with time and space. However, we consider this to be a modelling choice that will depend on the larger 2D or 3D model setup within which our parametrization would be applied, so we shall leave that to future work for now. Within this paper, we consider it sufficient that we have now demonstrated that by correctly setting the value of θ, we are able to more accurately predict the vertical mixing of buoyant particles.

We agree that it is a weakness of the KPP diffusion approach that KPP theory does not truly account for surface wave breaking, which can lead to significant mixing at the surface, as shown by Kukulka et al. (2012) and also our own SWB diffusion approach. Boufadel et al. (2020) suggested that the surface roughness z_0 could be used to account for surface wave breaking, and while this would require a lot more theoretical work with turbulence theory to prove or disclaim, the z_0 term does provide us with a simple way of testing the model sensitivity to high near-surface K_z values (as we state in lines 168 - 170). In our original formulation, we set z_0 according to Zhou &

Li (2019), which leads to $z_0 = 2.38 \times 10^{-6} - 2.86 \times 10^{-4}$ m. We now consider an alternative formulation where the roughness is a fraction of the significant wave height z_0=0.1Hs, where we calculate the significant wave height for a given wind condition according to Kukulka et al. (2012). This has minimal impact on the magnitude of K_z for depths greater than ~1 m, but does lead to higher K_z as $z \to 0$ (Figure B1). We show in figures 3, D1 and D2 that including this higher near-surface mixing can increase the depth to which particles are mixed below the surface, but overall, the effect is smaller than that of LC-driven mixing through θ. This agrees with the conclusions of Brunner et al. (2015) that LC turbulence has a stronger effect on the overall vertical concentration profiles than surface wave breaking does. As such, we conclude on lines 285 - 288 that: "although we recommend future work incorporating surface wave breaking into KPP theory, our current KPP diffusion approach representing LC-driving mixing through θ seems to capture the majority of turbulent mixing dynamics."

Kukulka, T., and K. Brunner. "Passive buoyant tracers in the ocean surface boundary layer: 1. Influence of equilibrium wind-waves on vertical distributions." *Journal of Geophysical Research: Oceans* 120.5 (2015): 3837-3858.

Brunner, K., et al. "Passive buoyant tracers in the ocean surface boundary layer: 2. Observations and simulations of microplastic marine debris." *Journal of Geophysical Research: Oceans* 120.11 (2015): 7559-7573.

McWilliams, James C., and Peter P. Sullivan. "Vertical mixing by Langmuir circulations." *Spill Science & Technology Bulletin* 6.3-4 (2000): 225-237.

Zhao, Dongliang, and Moxin Li. "Dependence of wind stress across an air–sea interface on wave states." *Journal of Oceanography* 75.3 (2019): 207-223.

Overall, this study does not add any new contributions to the field. The eddy diffusion profiles do not advance the state of the modelling, as they both have clear faults, and because they do not include all the relevant physics needed to fully explain the observations (Langmuir turbulence and/or breaking waves), it is hard to draw any conclusions from their comparisons to the data.

Vertical mixing can have a significant impact on the ultimate fate of buoyant particles in the ocean, and given that turbulence data from OGCMs is not readily available, we are convinced that our parametrizations provide a useful contribution to the modelling field. We would like to thank the reviewer for raising concerns about including all relevant physical processes, as we originally underestimated the influence of especially LC-driven mixing. We have now shown that by setting the Langmuir circulation enhancement term $\theta > 1.0$, our model can more accurately predict the depth to which buoyant particles are mixed with KPP diffusion. Properly accounting for surface wave breaking remains a weakness of KPP theory as a whole, but we have shown that the influence of such elevated near-surface K_z values on the overall vertical concentration profile is not as significant as with LC-driven mixing, such was also shown by Brunner et al. (2015). Therefore, we feel that our parametrizations do provide a useful, new contribution to the field, with our own documented model code being available to act as a foundation for any application of our parametrization to a larger 2D or 3D model setup.

Empirical Lagrangian parametrization for wind-driven mixing of buoyant particles at the ocean surface

Victor Onink[1,2,3], Erik van Sebille[3], and Charlotte Laufkötter[1,2]

[1]Climate and Environmental Physics, Physics Institute, University of Bern, Bern, Switzerland
[2]Oeschger Centre for Climate Change Research, University of Bern, Bern, Switzerland
[3]Institute for Marine and Atmospheric Research, Utrecht University, Utrecht, The Netherlands

Correspondence: Victor Onink (victor.onink@climate.unibe.ch)

Abstract. Turbulent mixing is a vital component of vertical particulate transport, but ocean global circulation models (OGCMs) generally have low resolution representations of near-surface mixing. Furthermore, turbulence data is often not provided in ~~reanalysis products~~OGCM model output. We present 1D parametrizations of wind-driven turbulent mixing in the ocean surface mixed layer, which are designed to be easily included in 3D Lagrangian model experiments. Stochastic transport is computed by Markov-0 or Markov-1 models, and we discuss the advantages/disadvantages of two vertical profiles for the vertical diffusion coefficient K_z. All vertical diffusion profiles and stochastic transport models lead to stable concentration profiles for buoyant particles, which for particles with rise velocities of 0.03 and 0.003 m s^{-1} agree relatively well with concentration profiles from field measurements of microplastics when Langmuir-circulation-driven turbulence is accounted for. Markov-0 models provide good model performance for integration timesteps of $\Delta t \approx 30$ seconds, and can be readily applied in studying the behaviour of buoyant particulates in the ocean. Markov-1 models do not consistently improve model performance relative to Markov-0 models, and require an additional parameter that is poorly constrained.

1 Introduction

Lagrangian models are essential tools to examine the transport of particulates in the ocean on a variety of spatial and temporal scales (Van Sebille et al., 2018), and have been used to study the movement of plastic particulates (Onink et al., 2019), oil (Samaras et al., 2014) and fish larvae (Paris et al., 2013). However, especially in the field of marine plastic modelling, most large scale modelling studies consider only virtual particles (henceforth referred to as particles) that float and remain at the ocean surface (Lebreton et al., 2018; Liubartseva et al., 2018; Onink et al., 2019, 2021), essentially simplifying the three dimensional ocean into a 2D system. While this does reduce the complexity of models, ultimately vertical transport processes need to be considered in order to have a complete understanding of oceanic particulate transport (Wichmann et al., 2019; Van Sebille et al., 2020).

In the case of buoyant particulates (particulates with a density lower than seawater), buoyancy is expected to return any particulates to the ocean surface. However, instead of all buoyant particulates accumulating at the ocean surface, both field measurements (Kukulka et al., 2012; Kooi et al., 2016b) and regional large-eddy simulations (LES) model studies (e.g. Liang et al., 2012; Yang et al., 2014; Brunner et al., 2015; Taylor, 2018) indicate vertical concentration profiles throughout the mixed layer (ML). These profiles arise due to the balance between the particulate buoyancy and turbulent mixing flows, which are largely driven by wind and wave breaking at the ocean surface (Chamecki et al., 2019). While such profiles are commonly used to correct surface measurements of particulates such as microplastics (e.g. Law et al., 2014; Egger et al., 2020), it is difficult to recreate such vertical mixing profiles in the ML outside of LES models, as vertical turbulent processes generally act on much smaller scales than is explicitly resolved in ocean global circulation models (OGCMs) (Taylor, 2018). In addition, while it is possible to represent mixing using the parametrization from Kukulka et al. (2012), this approach is only valid for depths up to several meters, while the mixed layer depth (MLD) can be hundreds of meters deep (Chamecki et al., 2019).

In this study we present numerical simulations of buoyant virtual particles in the ML with four 1D wind-driven mixing parametrizations. These mixing parametrizations have been specifically designed ~~for use in~~ such that the code can be easily adapted to function within large-scale 3D Lagrangian models running with OGCM data, for cases where the vertical spatial ~~scale~~ scales might be too coarse to explicitly represent turbulent processes or where turbulence data might not be provided as model output. Using these parametrizations we calculate the vertical equilibrium profiles of buoyant particles within the ML as a function of the particle rise velocities, the 10m wind speed and the MLD. Buoyant particles are found below the ML (Pieper et al., 2019; Choy et al., 2019; Egger et al., 2020), but diffusive mixing at such depths is likely not due to wind-driven turbulent mixing and therefore goes beyond the scope of this study. We test two methods for solving stochastic differential equations, and consider vertical diffusion coefficient profiles based on the KPP model (Large et al., 1994) and on Kukulka et al. (2012) extended by Poulain (2020). The modelled concentration profiles are then compared with measurements of vertical concentration profiles of microplastics.

2 Model Framework

2.1 Lagrangian stochastic transport

Turbulence in the ocean occurs over a wide range of spatial and temporal scales, with Kolmogorov length and timescales of $\eta = (\nu^3/\epsilon)^{1/4} = 3 \times 10^{-4}$ m and $\tau_n = (\nu/\epsilon)^{1/2} = 0.1$ s (Landahl and Christensen, 1998) for turbulent kinetic energy $\epsilon = 10^{-4}$ m^2 s^{-2} (Gaspar et al., 1990) and kinematic viscosity of seawater $\nu = 10^{-6}$ m^2 s^{-1} (Riisgård and Larsen, 2007). The vertical resolution of ~~OCGMs~~ OGCMs is typically on the order of meters and is therefore not capable of explicitly resolving all turbulent processes. Instead, turbulence due to sub-grid scale processes is generally represented stochastically. In our 1D vertical model, we simulate positively buoyant particles that are vertically transported due to stochastic turbulence and the particle rise velocity w_{rise}. For such particles, the particle trajectory $Z(t)$ can be computed with a stochastic differential

equation (SDE) (Gräwe et al., 2012) as:

$$Z(t+dt) = Z(t) + (w_{rise} + \partial_z K_z)dt + \sqrt{2K_z}dW \tag{1}$$

$$Z(0) = 0 \tag{2}$$

where $K_z = K_z\big(Z(t)\big)$ is the vertical diffusion coefficient, $\partial_z K_z = \partial K_z/\partial z$, dW is a Wiener increment with zero mean and variance dt and we define the vertical axis z as positive upward with $z = 0$ at the air–sea interface. The Euler-Maruyama (EM) scheme (Maruyama, 1955) is the simplest numerical approximation of equation 1, where infinitesimal terms dt and dW are replaced with the finite Δt and ΔW. Equation 1 can then be rewritten as (Gräwe et al., 2012):

$$w'(t) = \partial_z K_z + \frac{1}{\Delta t}\sqrt{2K_z}\Delta W \tag{3}$$

$$Z(t+\Delta t) = Z(t) + \big(w_{rise} + w'(t)\big)\Delta t \tag{4}$$

where w' is the stochastic velocity perturbation due to turbulence. The turbulent transport has both a deterministic drift term and a stochastic term. This is the most basic form of representing turbulent particle transport, as turbulent perturbations on the particle position are assumed to be uncorrelated (Berloff and McWilliams, 2003). The drift term assures that the well-mixed condition is met, which states that an initially uniform particle distribution must remain uniform even with inhomogeneous turbulence (Brickman and Smith, 2002; Ross and Sharples, 2004). This approach, termed a Markov-0 (M-0) or random walk model, assumes that turbulent fluctuations exhibit no autocorrelation on timescales Δt, which for global-scale Lagrangian simulations can range from 30 seconds (Lobelle et al., 2021) to 30 minutes (Onink et al., 2019). However, measurements from Lagrangian ocean floats show this is an oversimplification, as coherent oceanic flow structures can induce velocity autocorrelations that can persist for significantly longer timescales (Denman and Gargett, 1983; Brickman and Smith, 2002).

A higher order approach is the Markov-1 (M-1) model, which assumes a degree of autocorrelation of particle velocities set by the Lagrangian integral timescale T_L. The turbulent velocity perturbation is now expressed as a Langevin equation, and with an EM numerical scheme the particle trajectory $Z(t)$ is computed as (Mofakham and Ahmadi, 2020):

$$Z(t+\Delta t) = Z(t) + \big(w_{rise} + w'(t)\big)\Delta t \tag{5}$$

$$w'(t+\Delta t) = \alpha w'(t) + \partial_z \sigma_w^2 \Delta t + \sqrt{\frac{2(1-\alpha)\sigma_w^2}{\Delta t}}\Delta W \tag{6}$$

where $\alpha = 1 - \Delta t/T_L$ and $\sigma_w^2 = \sigma_w^2(z,t)$ is the variance of w', and we assume $\Delta t \leq T_L$. The influence of the initial turbulent fluctuations on subsequent fluctuations is set by α, which in turn depends on the ratio between the integration timestep Δt and T_L. However, empirical and theoretical estimates for T_L range from 6-7 seconds (Kukulka and Veron, 2019) to 15-30 minutes (Denman and Gargett, 1983), and T_L can also be depth dependent (Brickman and Smith, 2002). In large-eddy simulation (LES) models, $T_L = 4e/3C_0\epsilon$ where e is the sub-grid scale turbulent kinetic energy, C_0 is a model constant determining diffusion in the velocity space and ϵ is the turbulent kinetic energy dissipation rate (Kukulka and Veron, 2019), but e and ϵ are not commonly available variables in the output of OGCMs. However, it does indicate why model T_L estimates vary widely, as T_L describes

the autocorrelation of the particle velocity from its initial velocity due to unresolved sub-grid processes, which depends on the model resolution and setup in a given study. Since there is not a clear indication of the true value of T_L, we consider a range of values $\alpha \in [0, 0.1, 0.3, 0.5, 0.7, 0.95]$, corresponding to $T_L \in [1, 1.1, 1.4, 2, 3.3, 20] \times \Delta t$. As the depth dependence of T_L is uncertain, we make the simplification that $\partial_z T_L = \partial_z \alpha = 0$. Since $\Delta t \leq T_L$, we use $K_z = \sigma_w^2 \Delta t$ (Brickman and Smith, 2002), which means that equation 6 becomes:

$$w'(t) = \alpha w'(t) + \partial_z K_z + \frac{1}{dt}\sqrt{2(1-\alpha)K_z}\Delta W \tag{7}$$

In this form, it is clear that equation 7 is equivalent to equation 4 when $\alpha = 0$. This is because when $\alpha = 0$, velocity perturbations w' are assumed to be uncorrelated over timescales $\geq \Delta t$, which is equivalent to the M-0 formulation. M-1 stochastic models generally should lead to improved representation of diffusion in Lagrangian models (Berloff and McWilliams, 2003; Van Sebille et al., 2018), but it does require insight into turbulence statistics that have not yet been extensively studied in Lagrangian settings. For that reason, while even higher order Markov models are theoretically possible (Berloff and McWilliams, 2003), we limit this study to just the M-0 and M-1 approaches.

All Lagrangian simulations are run using Parcels v2.2.1 (Delandmeter and Sebille, 2019), ~~starting~~ which has been used for 1D, 2D and 3D particle oceanographic simulations (Fischer et al., 2021; Onink et al., 2021; Lobelle et al., 2021). The simulations start with 100,000 particles released at $Z(0) = 0$ and ~~running~~ run for 12 hours. The model is one dimensional with horizontal velocities set to zero. The time-invariant vertical diffusion profiles are calculated with a 0.1 m vertical resolution, where the K_z value at the exact particle location is linearly interpolated from these profiles. The vertical transport is calculated according to Equations 3 and 4 for M-0 simulations, and Equations 5 and 7 for M-1 simulations. We take $\Delta t = 30$ seconds, where the integration timestep is a compromise between accounting for turbulent transport on short timescales and computational cost for when the 1D model is integrated into a larger 3D Lagrangian model. We consider high, medium and low buoyancy particles with rise velocities of $w_{rise} \in [0.03, 0.003, 0.0003]$ m s^{-1}, which for plastic polyethylene ($\rho = 980$ kg m^{-3}) particles corresponds to spherical particles with diameters of 2.2, 0.4 and 0.1 mm (Enders et al., 2015). However, these particle sizes are rough indications of approximate particle sizes, as the buoyancy of particle depends on a combination of the particle size, shape, polymer density and degree of biofouling (Kooi et al., 2016b; Brignac et al., 2019; Kaiser et al., 2017). Relative to peak stochastic velocity perturbations w' calculated from the vertical diffusion coefficients described in Section 2.2, the rise velocity of the high buoyancy particles dominate w' except for the highest wind speeds, while turbulence dominates buoyancy for the medium and low buoyancy particles for almost all wind conditions (Table A1). The surface wind stress is computed from $u_{10} \in [0.85, 2.4, 4.35, 6.65, 9.3]$ m s^{-1}. The model domain is $z \in [-100, 0]$m, where we apply a ceiling boundary condition (BC) in which particles that cross the surface boundary are placed at $z = 0$. This BC assures that neither buoyancy or turbulence can transport particles out of the water column. Vertical concentration profiles are computed by binning the final particle locations into ~~0.2~~ 0.5 m bins, and the concentrations are then normalized by the total number of particles in the simulation. The variability of the profiles at each depth level is calculated as the standard deviation over the final hour of each simulation.

2.2 Vertical diffusion profiles

Two vertical diffusion coefficient profiles are used, with the first based on Kukulka et al. (2012) and Poulain (2020). Kukulka et al. (2012) parametrized the near-surface vertical diffusion coefficient K_z^S due to breaking waves as:

$$K_z^S = 1.5 u_{*w} \kappa H_s \tag{8}$$

for $z > -1.5H_s$, where $\kappa = 0.4$ is the von Karman constant, H_s is the significant wave height and u_{*w} is the ~~frictional~~ friction velocity of water. The significant wave height H_s is parametrized as ~~$H_S = 0.96 g^{-1} \beta_*^{3/2} u_{*a}^2$~~ $H_s = 0.96 g^{-1} \beta_*^{3/2} u_{*a}^2$, where $g = 9.81$ m s^{-2} is the accelation of gravity, $\beta_* = c_p / u_{*a}$ is the wave age, c_p being the characteristic phase speed of the surface waves and $u_{*a} = \tau / \rho_a$ is the ~~frictional~~ friction velocity of water. The ~~frictional~~ friction velocity of air is based on the air density $\rho_a = 1.22$ kg m^{-3} and the surface wind stress $\tau = C_D \rho_a u_{10}^2$, where u_{10} is the 10m wind speed and C_D is the drag coefficient (Large and Pond, 1981). Similarly, $u_{*w} = \tau / \rho_w$ with the seawater density $\rho_w = 1027$ kg m^{-3}. Following Kukulka et al. (2012), we assume a fully developed sea-state with $\beta_* = 35$. The Kukulka et al. (2012) parametrization is valid only for $z \approx -1.5H_s$, and we extend the parametrization for greater depths using the eddy viscosity profile ν_z as found for oscillating grid turbulence by Poulain (2020):

$$\nu_z = \begin{cases} \nu^S \text{ if } z > -H_s \\ \nu^S H_s^{3/2} |z|^{-3/2} \text{ if } z < -H_s \end{cases} \tag{9}$$

where ν^S is the near surface eddy viscosity. This approach agrees with Kukulka et al. (2012) in predicting constant mixing for $z > -H_s$, where the eddy viscosity then drops proportional to $z^{-3/2}$ for greater depths. Oscillating grid turbulence (OGT) experiments are commonly used to study wave and wind induced turbulence (Fernando, 1991)~~, and~~ . As OGT experiments have been shown to reproduce turbulence decay laws of velocities and dissipation rates ~~found~~ observed in the ocean ML (Thompson and Turner, 1975; Hopfinger and Toly, 1976; Craig and Banner, 1994), this provides some confidence in the modelling of the decay of near-surface eddy viscosity, although direct validation with field measurements of eddy viscosity have yet to occur. The diffusion coefficient K_z depends on ν_z as $K_z = \nu_z / Sc_t$, where Sc_t is the turbulent Schmidt number, and assuming $\partial_z Sc_t = 0$, combining equations 8 and 9 results in:

$$K_z = \begin{cases} K_z^S + K_B = 1.5 u_{*w} \kappa H_s + K_B \text{ if } z > -H_s \\ K_z^S H_s^{3/2} |z|^{-3/2} + K_B = 1.5 u_{*w} \kappa H_s^{5/2} |z|^{-3/2} + K_B \text{ if } z < -H_s \end{cases} \tag{10}$$

where $K_B = 3 \times 10^{-5}$ m^2 s^{-1} is the dianeutral diffusion below the MLD (Waterhouse et al., 2014). The diffusion is thus constant for $z > -H_s$, below which $K_z \propto |z|^{-3/2}$, while the magnitude of K_z increases for higher wind speeds (Fig. 1). As $z \to -\infty$, $|z|^{-3/2} \to 0$, and therefore we include the bulk dianeutral diffusion K_B to account for vertical mixing at depths below the influence of surface wave-driven turbulence. As both Kukulka et al. (2012) and Poulain et al. (2018) considered turbulence generated by breaking surface waves, we refer to this diffusion approach as Surface Wave Breaking (SWB) diffusion.

The second vertical diffusion coefficient profile is a local form of the K-profile parameterization (KPP) (Large et al., 1994; Boufadel et al., 2020), where K_z is given by:

$$K_z = \left(\frac{\kappa u_{*w}}{\phi}\theta\right)(|z| + z_0)\left(1 - \frac{|z|}{MLD}\right) + K_B \tag{11}$$

where $\phi = 0.9$ is the "stability function" of the Monin-Obukov boundary layer theory, ~~$\theta = 1$~~ θ is a Langmuir circulation (LC) enhancement factor, and z_0 is the roughness scale of turbulence. As such, K_Z rises from a small non-zero value at $z = 0$ to a maxima at $z = 1/3MLD$, before dropping to $K_z = K_B$ for $z \leq MLD$ (Fig. 1). In the original KPP formulation $K_z(z \leq MLD) = 0$ since the theory only applies to the surface mixed layer, so we add the same bulk dianeutral diffusion term K_B as with the SWB profile (equation 10). Boufadel et al. (2020) examined a case where LC-driven turbulence was considered negligible and so $\theta = 1.0$. However, the presence of LC can increase turbulent mixing by a factor $\theta = 3 - 4$ (McWilliams and Sullivan, 2000) and has been shown to strongly affect the vertical concentration profiles of buoyant microplastic particles in LES experiments (Brunner et al., 2015; Kukulka and Brunner, 2015). Therefore, we examine $\theta \in [1.0, 2.0, 3.0, 4.0, 5.0]$.

The roughness scale z_0, which can represent the surface roughness due to surface waves, depends on the wind speed and the wave age (Zhao and Li, 2019), and following Kukulka et al. (2012) we consider a wave age $\beta_* = c_p/u_{*a} = 35$ that is equivalent to $\beta = c_p/u_{10} = 1.21$. ~~Following~~ According to Zhao and Li (2019), the roughness scale is given by:

$$z_0 = 3.5153 \times 10^{-5}\beta^{-0.42}u_{10}^2/g \tag{12}$$

~~The~~ For $w_{10} = 0.85 - 9.30$ m s^{-1}, this means $z_0 = 2.38 \times 10^{-6} - 2.86 \times 10^{-4}$ m. To test the model sensitivity to z_0, we also consider an alternative scenario where $z_0 = 0.1 \times H_s = 1.76 \times 10^{-3} - 2.10 \times 10^{-1}$ m, following the same formulation $H_s = 0.96g^{-1}\beta_*^{3/2}u_{*a}^2$ as in Kukulka et al. (2012). This increases K_z for $z \approx 0$, but does not significantly affect the magnitude K_z at greater depths (Figure B1). The original KPP theory does not explicitly account for surface wave breaking, which would lead to larger non-zero K_z at $z = 0$. While we do not claim that setting $z_0 = 0.1 \times H_s$ means that our KPP profile accounts for surface wave breaking turbulent mixing, it allows us to investigate the influence higher near-surface mixing would have on the modelled vertical concentration profiles. The MLD is the maximum depth of the surface ocean boundary layer formed due to interaction with the atmosphere, and in KPP theory the MLD is defined as the depth where the bulk Richardson number Ri_B is first equal to a critical value Ri_{crit}. In the original formulation $Ri_{crit} = 0.3$ (Large et al., 1994), but Ri_B can be difficult to compute in the field as this requires data for both vertical density and velocity shear profiles. In this study we prescribe MLD= 20 m, as this falls within the range of the MLD for field data used to evaluate the model (see Section 2.3). ~~Since KPP theory predicts $K_z = 0$ if $z < -$MLD, we add the same bulk dianeutral diffusion term K_B as with the SWB profile (equation 10).~~

2.3 Field data

We compiled a dataset of vertical plastic concentration profiles collected within the surface mixing layer to validate the modelled concentration profiles (Table 1), with a total of 90 profiles with 741 data points. Only Kooi et al. (2016b) ~~reported~~ directly measured the rise velocity of a subsample of the collected microplastic particulates, and showed that these particles were

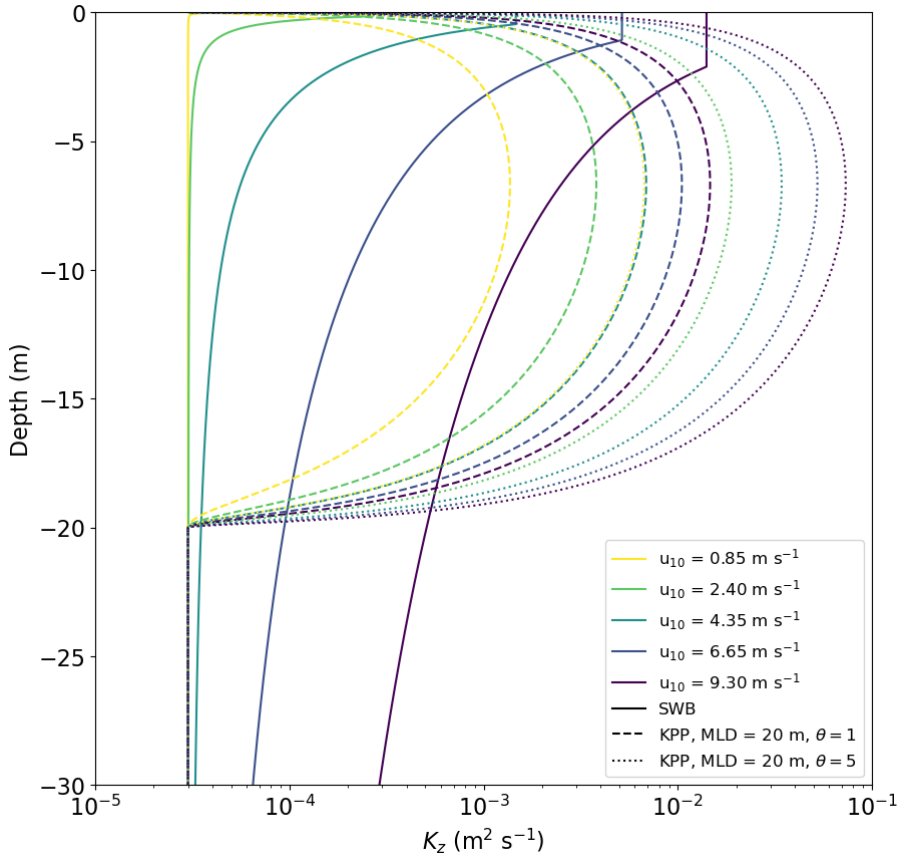

Figure 1. Vertical diffusion coefficient profiles for SWB and KPP diffusion under varying wind conditions. The KPP diffusion profile is calculated with z_0 according to Equation 12.

positively buoyant. However, the presence of all the other sampled particulates near the open ocean surface indicates they are unlikely to be negatively buoyant. For all stations the wind speed was recorded and the MLD was determined from CTD data based on a temperature threshold (de Boyer Montégut et al., 2004). The majority of samples were collected in the North Atlantic (Kukulka et al., 2012; Kooi et al., 2016b; Pieper et al., 2019), and in regions with a relatively shallow MLD. Since wind-driven turbulent mixing isn't expected to influence the concentration depth profile below the MLD, we don't consider any measurements collected below 73 m. Measurements were collected with surface wind speeds up to 10.7 m s^{-1}, with the majority of sampled concentrations being collected for $u_{10} = 3.4 - 7.9$ m s^{-1} (535/741 data points).

Almost all measurements were collected with neuston nets, either multi-level nets simultaneously sampling fixed depth intervals (Kooi et al., 2016b) or using multi-stage nets that consecutively sample fixed depths or depth ranges (Kukulka et al. (2012); Egger et al. (2020); Amaral-Zettler (unpublished data)). These nets have mesh-sizes of 0.33 mm, and will generally

Table 1. Overview of the sources of field measurements of microplastic concentration profiles. The uncertainty in the mean MLD is the standard deviation.

Source	Measurement Approach	Number of concentration profiles	Number of data points	Mean MLD [min max] (z)
Kooi et al. (2016b)	Neuston net	46	506	15.4±3.6 [10.0, 26.2]
Pieper et al. (2019)	Niskin bottles	12	152	17.1±5.5 [11.0, 28.0]
Kukulka et al. (2012)	Neuston net	13	47	24.3±8.9 [11.0, 45.1]
Egger et al. (2020)	Neuston net	16	20	55.8±19.2 [12.3, 72.8]
Amaral-Zettler (unpublished data)	Neuston net	3	16	17.8±4.8 [14.0, 26.0]
Total		90	741	17.5±8.8 [10.0, 72.8]

sample high and medium ($w_{rise} = 0.03 - 0.003$ m s^{-1}) buoyancy particulates, which for non-biofouled polyethylene would have a diameter greater than the mesh size (2.2 and 0.4 mm). In contrast, low buoyancy particulates ($w_{rise} = 0.0003$ m s^{-1}) are typically not sampled in neuston nets (Kooi et al., 2016b), likely in part due to smaller particulate sizes. Pieper et al. (2019) filtered samples collected via Niskin bottles with a 0.8μm filter and thus was able to filter out smaller particulates with lower rise velocities.

All measured microplastic concentrations are normalized by total amount of plastic measured within a vertical profile. In order to compare the average normalized field concentration with the modelled profiles, we bin the normalized field concentrations into 0.5 m depth bins and calculate the standard deviation for each depth bin. Comparison of the modelled concentration profiles with the binned normalized field measurements is done via the root mean square error (RMSE):

$$RMSE = \sqrt{\frac{1}{n}\sum_{i=0}^{n}(C_{f,i} - C_{m,i})} \tag{13}$$

where $C_{f,i}$ and $C_{m,i}$ are the binned normalized field measurement and modelled concentration within depth bin i. Model evaluation for the low buoyancy particles is not possible with the available field measurements as low buoyancy particles are typically too small to be sampled with neuston nets, and the Pieper et al. (2019) dataset alone is too small.

3 Results

Starting with all particles at $z = 0$ for $t = 0$, M-0 models with both KPP and SWB diffusion lead to stable vertical concentration profiles ~~within 12 hours~~ (Fig. 2), where the equilibrium concentration profile is already established within 1 - 2 ~~or 3 hours .~~ hours (Fig. C1). For both diffusion profiles, ~~increased wind speeds lead to greater downward mixing of the particles . However, with SWB diffusion the~~ there is progressively deeper mixing of particles with increasing wind speeds and decreasing

buoyancy. While with both SWB and KPP diffusion low buoyancy particles always get mixed below the surface, for medium and high buoyancy particles there exist minimum wind speeds below which all particles remain at the surface~~until $w_{10} \geq 9.30$~~ . These limits are similar for both diffusion types for medium buoyancy particles ($u_{10} \geq 2.40$ m s^{-1}~~while with KPP diffusion~~), but high buoyancy particles ~~always remain at the surface . Less buoyant particles get mixed deeper into the water column, as turbulent mixing forces dominate over the particle rise velocity.~~ only mix below the surface with SWB diffusion if $u_{10} \geq 9.30$ m s^{-1}. However, once mixing below the ocean surface occurs, KPP diffusion always leads to deeper mixing of particles than SWB diffusion due to higher subsurface K_z values.

The concentration profiles for medium and low buoyancy particles are largely unaffected by reducing Δt below 30 seconds (Fig. E1). However, for high buoyancy particles with SWB diffusion the concentration profile more strongly depends on Δt due to the applied boundary condition. For $\Delta t = 30$ s, the M-0 model shows all particles remain near the ocean surface, but shorter Δt values indicate that ~~downward mixing~~ deeper mixing of particles already occurs for $u_{10} = 6.65$ m s^{-1}. ~~For~~ With KPP diffusion, all high buoyancy particles ~~, the concentration profiles with KPP and SWB diffusion are very similar, with SWB generally leading to slightly deeper mixing due to the higher near-surface~~ remain at the surface even with $\Delta t = 1$ second, as K_z ~~values (Fig. 1). However, for~~ at $z = 0$ remains too low to overcome the high rise velocity.

Even though KPP diffusion with $\theta = 1.0$ and z_0 following (Zhao and Li, 2019) predicts deeper mixing of particles than with SWB diffusion, both approaches underpredict the mixing of particles relative to field observations. For KPP diffusion, this can be corrected by accounting for LC-driven mixing, which leads to deeper mixing of particles for both medium and low buoyancy particles ~~KPP diffusion leads to greater downward mixing compared to SWB diffusion. The decreased buoyancy slows the particle rise to the surface, and for $z \lessapprox -H_s$ KPP diffusion generally has higher K_z values than SWB diffusion. For the low buoyancy particles , this leads to uniform concentrations in the ML for $w_{rise} > 4.35$ m s^{-1}.Both SWB and KPP diffusion lead to concentration profiles that match reasonably well with observations, with similar RMSE values relative to field measurements for given wind conditions (Fig.~~ (Figures 3 & D1). For medium buoyancy particles this generally leads to better model agreement with lower RMSE values between the modelled and averaged field data concentration profiles (Figure 4). ~~Model evaluation for the low buoyancy particles is not possible with the available field measurements as low buoyancy particles are typically too small to be sampled with neuston nets.~~ However, for high buoyancy particles LC-driven circulation is not enough as particles remain at the ocean surface for all wind conditions even for $\theta = 5.0$ (Figure D2), as K_z for $z \approx 0$ is too low to overcome the inherent particle buoyancy. Only when LC-driven is combined with higher near-surface K_z values by setting $z_0 = 0.1 \times H_s$ do we see any below-surface mixing of high buoyancy particles when $\theta > 3.0$ and $u_{10} \geq 9.30$ m s^{-1}. Increased near-surface K_z values have a lesser influence on the concentration profiles of medium and low density particles, as these particles were already being mixed below the surface even without larger z_0 values.

With both KPP and SWB diffusion, M-1 models show ~~increased leads to increased downward~~ deeper mixing of particles ~~with increasing α~~ as $\alpha \to 1$ (Fig. 5). Relative to the field measurements, M-1 models can at best slightly improve model performance

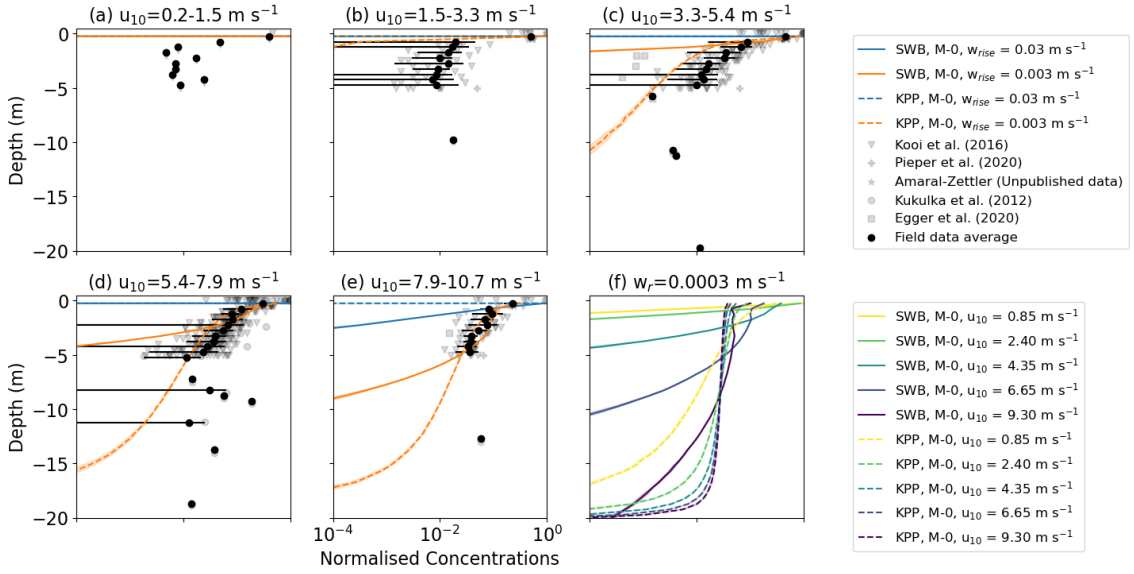

Figure 2. Vertical concentrations of buoyant particles for KPP and SWB diffusion using M-0 models. Subfigures (a) - (e) show the vertical concentration profiles for high and medium buoyancy particles with increasing wind speeds. The KPP profiles are calculated for $\theta = 1.0$ and z_0 according to Equation 12. The grey markers indicate field measurements, with darker shades indicating more measurements, while the binned field measurement average and standard deviation are shown by the black markers. Subfigure (f) shows the vertical concentration profiles for low buoyancy particles under increasing wind conditions. Shading around the profiles indicates the profile's standard deviation at each depth level.

over M-0 models (Fig. 6). However, improved model performance is not shown across all particle sizes and wind conditions, and there is not a consistent α value leading to the smallest RMSE values.

4 Discussion

The parametrizations presented in this study are intended for use in 3D Lagrangian experiments using OGCM data, and therefore should yield numerically stable results for the relatively large integration timesteps used in large-scale Lagrangian vertical transport modelling (Lobelle et al., 2021). While there are more stable schemes available than the EM scheme used in this study (Gräwe et al., 2012), the EM scheme is computationally the cheapest and yields concentration profiles that match reasonably well with observations. Both M-0 and M-1 models show largely convergent concentration profiles for $\Delta t = 30$ seconds, which would make both approaches feasible with regards to computational cost. However, we would currently recommend using a M-0 model. M-1 models have the additional tuning parameter α representing the autocorrelation of turbulent velocity fluctuations, which is poorly constrained in the literature. Using spatially invariant α values at best slightly improved model performance in comparison with M-0 models, and constraining α is not possible from these results. M-1 models may improve modelling of vertical diffusive transport, but more work is required to further constrain the value and vertical profile of α. Finally, numer-

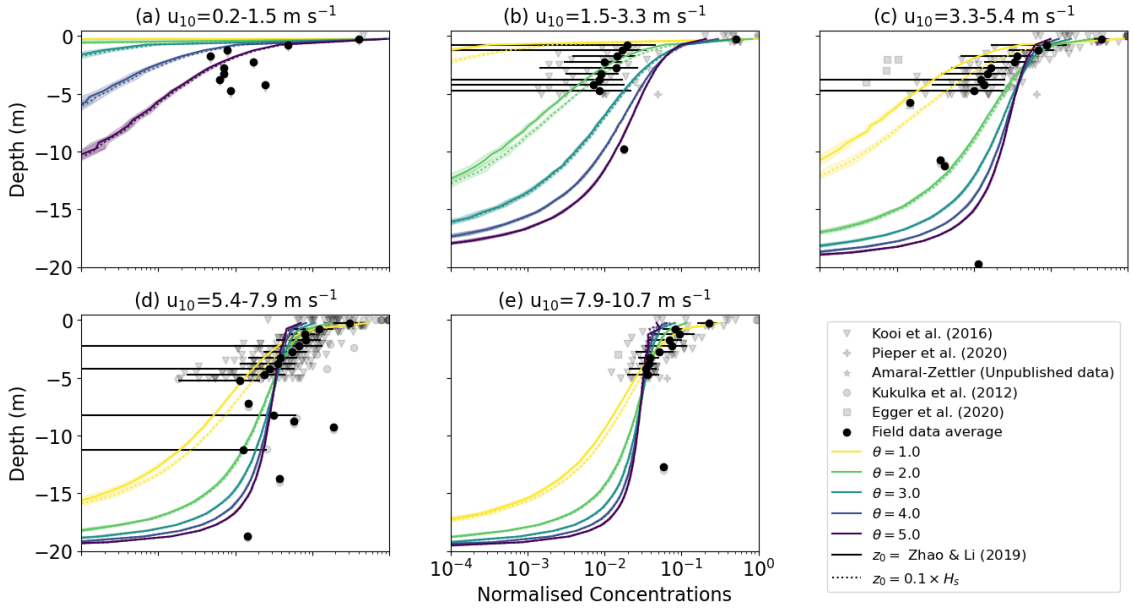

Figure 3. ~~RMSE between field measurements and modelled concentration profiles~~ Vertical concentrations of buoyant particles for KPP diffusion using M-0 models ~~with~~ for $w_r = 0.003$ m s^{-1}. The KPP profiles are calculated for $\theta = [1.0, 2.0, 3.0, 4.0, 5.0]$ and ~~SWB diffusion under different wind conditions~~with either $z_0 = 0.1 \times H_s$ or according to Equation 12. The grey markers indicate field measurements, with darker shades indicating more measurements, while the binned field measurement average and standard deviation are shown by the black markers. Shading around the profiles indicates the profile's standard deviation at each depth level.

ous formulations of the M-1 drift term have been proposed (Mofakham and Ahmadi, 2020; Brickman and Smith, 2002, e.g.) which can lead to large differences in the modelled profiles. In this study we used the non-normalized Langevin equation from Mofakham and Ahmadi (2020), but other formulations could be explored in future work.

While the concentration profiles of medium and low buoyancy particles are unaffected by decreasing the integration timestep $\Delta t < 30$ seconds, using higher Δt values underestimates the ~~downward mixing~~ depth to which high buoyancy particles are mixed when using SWB diffusion. This is because for high Δt values, the upward non-stochastic component of equation 6, which scales with Δt, dominates the stochastic component, which scales with $\sqrt{\Delta t}$. With KPP diffusion the vertical profile for high buoyancy particles appears unaffected by Δt, but this is ~~just~~ because the near-surface K_z values are significantly lower than with SWB diffusion. One possibility to correct for this is to apply a different BC, such as a reflective BC. While the concentration profiles for medium and low buoyancy particles are not strongly affected by such a reflective BC (Fig. F1), the reflective BC does show ~~greater downward~~ deeper particle mixing with SWB diffusion. However, for $\Delta t = 30$ seconds the ~~downward~~ depth of mixing is now overestimated compared to smaller Δt values (Fig. F2), ~~while~~ as with $\Delta t = 30$ seconds and $w_r = 0.03$ m s^{-1} the particle would by reflected up to 0.9 m below the ocean surface solely due to the model numerics. In

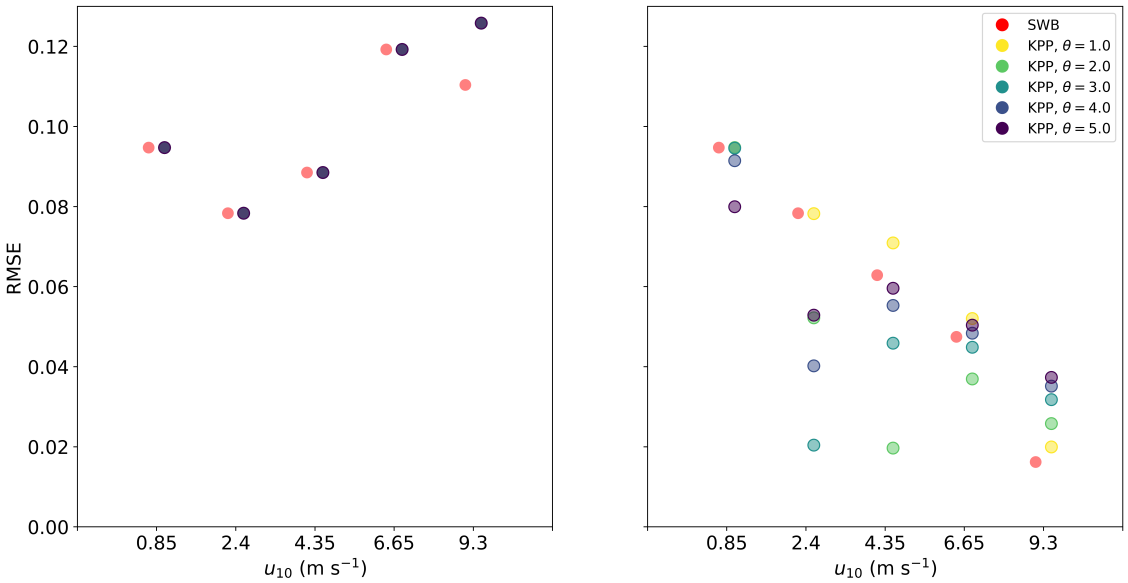

Figure 4. RMSE between field measurements and modelled concentration profiles for M-0 models with KPP and SWB diffusion under different wind conditions. All KPP diffusion simulations were with z_0 according to Equation 12.

addition, earlier studies have shown that reflecting BC can cause spurious increases in particle concentration near the boundary (Ross and Sharples, 2004; Nordam et al., 2019). Therefore, changing the BC to a reflective BC would not improve the concentration profiles of high buoyancy particles. Depending on the model application and setup, the error in the concentration profile depth ($\mathcal{O}(1)$ m for high buoyancy particles) might be acceptable. Otherwise, the error can be reduced by using a smaller integration timestep where that is computationally feasible.

Considering the KPP and SWB diffusion profiles, the results in this study ~~are inconclusive with regards to which approach is superior~~indicate that KPP diffusion generally performs better relative to field observations. For high buoyancy particles, SWB diffusion leads to slightly deeper particle mixing, ~~but model performance is generally very similar. With~~ while only if the KPP diffusion profile accounts for LC-driven turbulence and has higher near-surface K_z values can it similarly show below-surface mixing of high buoyancy particles for $u_{10} \geq 9.30$ m s^{-1}. However, with medium and low buoyancy particles the KPP profile leads to much deeper mixing, ~~but it is difficult to evaluate whether this is a more realistic concentration profile . The majority of the~~ especially when accounting for LC-driven turbulence, and this appears to agree better with field observations. As with (Brunner et al., 2015), we see that elevated near-surface K_z values due to e.g. wave breaking have a comparably smaller influence on the overall concentration profile than LC-driven mixing, as similarly shown by (Brunner et al., 2015). Therefore, although we recommend future work incorporating surface wave breaking into KPP theory, our current KPP diffusion approach representing LC-driving mixing through θ seems to capture the majority of turbulent mixing dynamics. It must be noted though that the majority of the field measurements are collected in the top 5 meters of the water column, and more measurements would

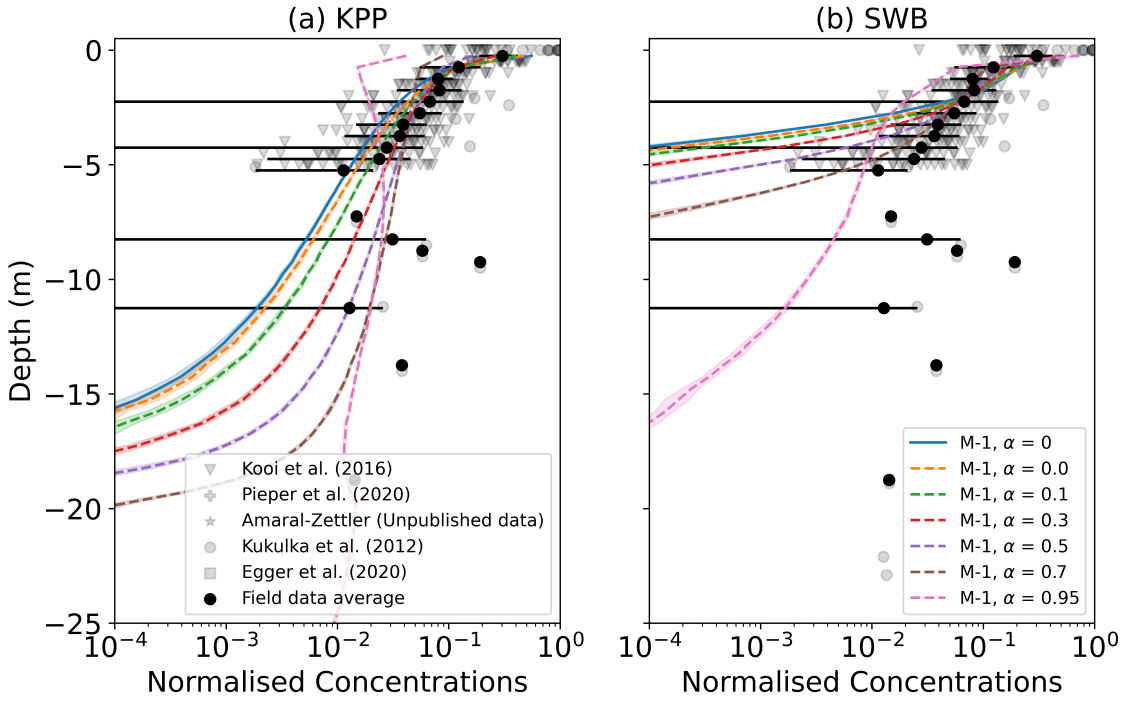

Figure 5. Vertical concentrations of buoyant particles for (a) KPP and (b) SWB diffusion using M-0 and M-1 models with varying values for α. The grey markers indicate field measurements, with darker shades indicating more measurements, while the binned field measurement average and standard deviation are shown by the black markers. Shading around the profiles indicates the profile's standard deviation at each depth level. The KPP profiles are for $\theta = 1.0$ and z_0 according to 12. All profiles are for $u_{10} = 6.65$ m s^{-1} and medium buoyancy particles ($w_{rise} = 0.003$ m s^{-1}).

need to be collected at greater depths to ~~evaluate how many~~ further evaluate the depth to which medium-buoyancy particles are mixed~~further down. The~~ . In addition, the currently available data collected with Neuston nets does not allow for model evaluation for the low-buoyancy particles. As such, more field measurements (including smaller-sized particles) would be necessary to ~~distinguish which diffusion profile leads to the most realistic concentration profiles.~~ fully evaluate model performance for all particles sizes with the two diffusion profiles.

With regards to necessary data to calculate the diffusion profiles, the SWB approach has the benefit that it only requires surface wind stress data, while KPP diffusion additionally requires MLD data. ~~In contrast, since KPP diffusion is commonly used in OCGMs (Boufadel et al., 2020), using this would mean that vertical particle transport is consistent with other model tracers. In addition~~Furthermore, our results indicate that accounting for LC-driven turbulent mixing improves KPP diffusion model performance, but determining which θ value to use is not trivial. McWilliams and Sullivan (2000) demonstrated that θ is inversely proportional to the Langmuir number La, which is defined as $La = \sqrt{u_{*w}/U_S}$ with U_S as the surface Stokes drift.

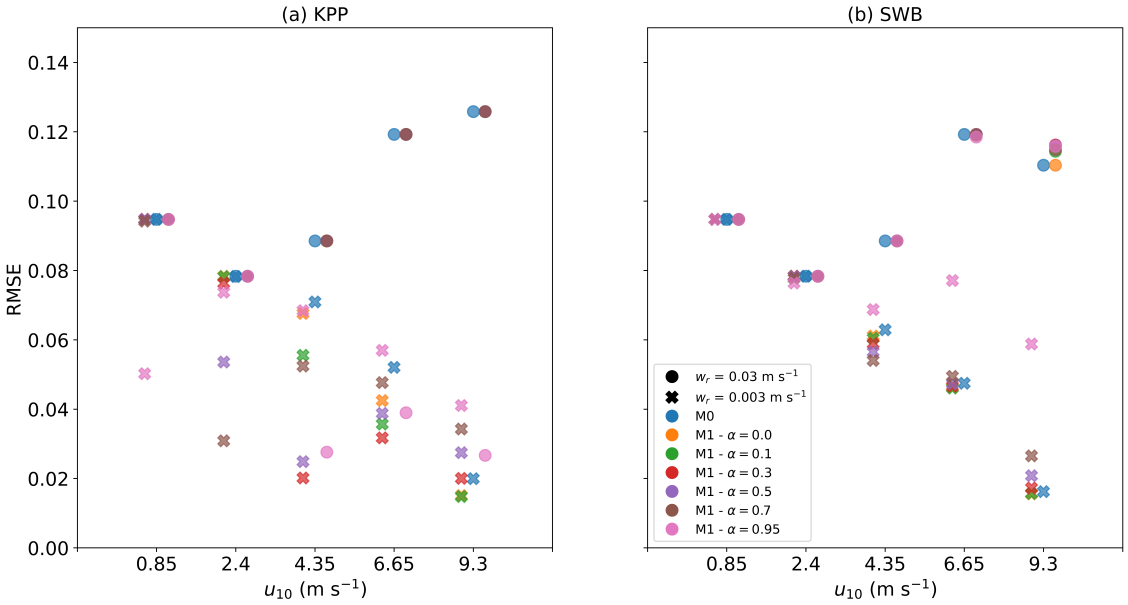

Figure 6. RMSE between field measurements and modelled concentration profiles for M-0 and M-1 models with (a) KPP and (b) SWB diffusion under different wind conditions and with varying values of α. All KPP diffusion simulations were with $\theta = 1.0$ and z_0 according to 12.

The Langmuir number can conceivably be calculated using OGCM data, but the details of such an implementation will be left for future work with 3D Lagrangian models. Furthermore, KPP diffusion has the advantage that it has been widely used and validated in various model setups (Boufadel et al., 2020; McWilliams and Sullivan, 2000; Large et al., 1994), while such extensive validation has not yet occured for SWB diffusion. Finally, the influence of wind forcing on turbulence is generally assumed to be limited to the surface mixed layer (Chamecki et al., 2019), while with the SWB profile wind-generated turbulence can extend below the MLD. To represent sub-MLD mixing, either a constant K_z value or other K_z profiles could be used, such as the K_z estimates for internal tide mixing as proposed by de Lavergne et al. (2020).

In all cases, the vertical concentration profiles stabilized to vertical equilibrium profiles, similar to what has been shown for buoyant particles in LES model studies (Liang et al., 2012; Yang et al., 2014; Brunner et al., 2015; Taylor, 2018). The modelled concentration profiles generally resembled the profiles from field measurements of microplastic concentrations under different wind conditions (Kooi et al., 2016b; Kukulka et al., 2012), but the averaged concentration profiles of the field measurements are quite noisy. Partly, this could be due to inhomogeneity in the particle buoyancy, as the collected microplastic particulates have varying sizes and rise velocities (Kooi et al., 2016b; Egger et al., 2020). Additionally, we sorted the field measurements based on wind conditions, but other underlying oceanographic conditions such as the MLD can still vary significantly even with similar wind speeds. ~~Furthermore, for the model simulations we assumed~~ Unfortunately, we lack additional data of the

oceanographic conditions at the of sampling, which currently prohibits more high-level comparisons of the field and model concentration profiles. Compared with the field data, the variance in the modelled concentration profiles is significantly smaller. This is in part also due to assuming constant environmental conditions over 12 hours ~~, but~~ for the model simulations, while e.g. wind conditions can change on much shorter timescales over the ocean surface. To further improve vertical transport model verification, more measurements would be required, covering a wider range of oceanographic conditions (such as for wind conditions higher than $u_{10} = 10.7$ m s^{-1}) and with a high spatial sampling resolution also for depths $z < -5$m. Ideally these measurements would also sample small, neutrally buoyant particulates, but we acknowledge this is difficult with the sampling techniques commonly used today. At the same time, we would encourage conducting more ocean field measurements of near-surface vertical eddy diffusion coefficient and/or eddy viscosity profiles, as this will allow further validation of the K_z profiles predicted by the KPP and SWB theory with actual ocean near-surface mixing measurements.

The parameterizations have been validated for high/medium rise velocities~~. However, they should also apply to neutral or negatively buoyant particles, as the SWB and KPP profiles estimate the amount of turbulence in the water column irregardless of the types~~ , and at least for KPP diffusion with $\theta > 1.0$ the concentration profiles resemble those calculated from field observations. This provides confidence in the turbulence estimates from the KPP approach, and as these are independent of the type of particle that might be present~~. Given that~~ , this would suggest the KPP approach can also be applied to to neutral or negatively buoyant particles. However, as model verification was only possible for microplastic particulates with rise velocities approximately between 0.03 - 0.003 m s^{-1}, we would advise additional model verification for other particle types where the necessary field data is available. In the case of SWB diffusion, turbulent mixing seems underestimated when further from the ocean surface, and we would advise more validation with field observations before applying this diffusion approach to other particle types.

5 Conclusions

We have developed a number of 1D surface-mixing parametrizations designed to be readily applied in large-scale oceanic Lagrangian model experiments using ~~OCGM~~ OGCM data. Where possible, we would recommend using the turbulence fields from the ~~OCGM~~ OGCM to assure turbulent transport of the particles is consistent with that of other model tracers. However, if the turbulence fields are unavailable then ~~these parametrizations~~ particularly parametrizations with KPP diffusion with LC-driven mixing are shown to produce modelled vertical concentration profiles that match relatively well with field observations of microplastics. The parametrizations generally perform well for timesteps of $\Delta t = 30$ seconds, but for high buoyancy particles users need to take care to use sufficiently short timesteps, especially with SWB diffusion. Verification was only possible for positively buoyant particles larger than 0.33 mm (which generally have rise velocities ≤ 0.003 m s^{-1}), but the parametrizations should also be applicable to other particle types. The parametrizations can therefore be applied to investigate the influence of turbulent mixing on the vertical transport of (microplastic) particles within a 3D model setup, and ultimately gain a more complete understanding of the fate of such particles in the ocean.

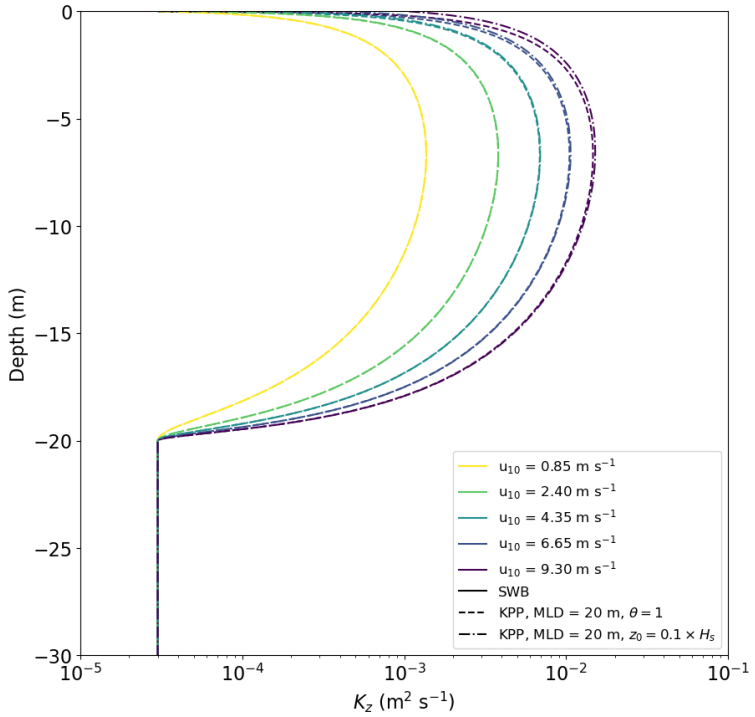

Figure B1. Vertical diffusion coefficient profiles for KPP diffusion under varying wind conditions with $\theta = 1.0$. The KPP diffusion profile is calculated either with z_0 according to Equation 12 or $z_0 = 0.1 \times H_s$.

6 Code and data availability

The code for the 1D model, the subsequent analysis and all figures is available at zenodo (Onink, 2021). The field data for Kooi et al. (2016b) is available at figshare (Kooi et al., 2016a). For the field data from Kukulka et al. (2012), Pieper et al. (2019), Egger et al. (2020) and Amaral-Zettler (unpublished data), please contact the corresponding authors of the respective studies.

Table A1. Ratios w_r/w' between the rise velocity w_r and the peak stochastic velocity perturbation w' for KPP and SWB diffusion. The peak w' is the maximum value of Equation 3. The peak w' values for KPP diffusion are calculated for $\theta \in [1.0, 3.05.0]$ and for z_0 following Equation 12.

Wind Speed (m s^{-1})	Diffusion Type	$w_r = 0.03$ m s^{-1}	$w_r = 0.003$ m s^{-1}	$w_r = 0.0003$ m s^{-1}
0.85	KPP, $\theta = 1.0$	1.818	0.182	0.018
	KPP, $\theta = 3.0$	1.055	0.106	0.011
	KPP, $\theta = 5.0$	0.818	0.082	0.008
	SWB	10.512	1.051	0.105
2.40	KPP, $\theta = 1.0$	1.087	0.109	0.011
	KPP, $\theta = 3.0$	0.628	0.063	0.006
	KPP, $\theta = 5.0$	0.486	0.049	0.005
	SWB	4.077	0.408	0.041
4.35	KPP, $\theta = 1.0$	0.808	0.081	0.008
	KPP, $\theta = 3.0$	0.465	0.047	0.005
	KPP, $\theta = 5.0$	0.359	0.036	0.004
	SWB	1.753	0.175	0.018
6.65	KPP, $\theta = 1.0$	0.654	0.065	0.007
	KPP, $\theta = 3.0$	0.373	0.037	0.004
	KPP, $\theta = 5.0$	0.288	0.029	0.003
	SWB	0.935	0.094	0.009
9.30	KPP, $\theta = 1.0$	0.553	0.055	0.006
	KPP, $\theta = 3.0$	0.313	0.031	0.003
	KPP, $\theta = 5.0$	0.241	0.024	0.002
	SWB	0.566	0.057	0.006

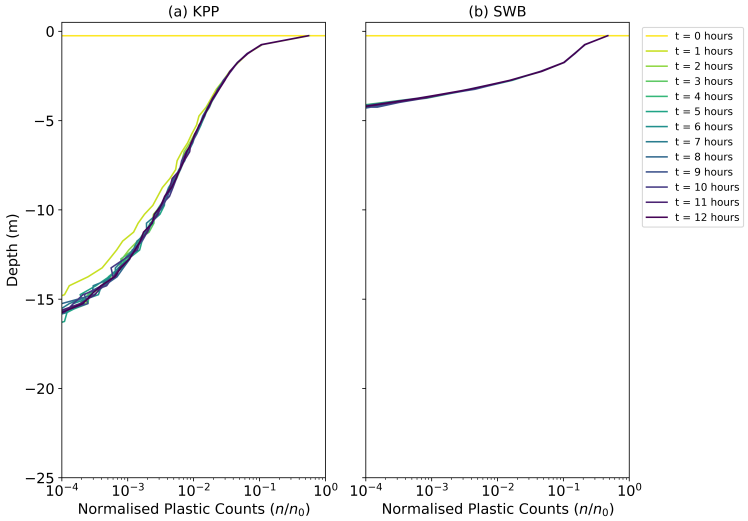

Figure C1. Vertical concentrations of buoyant particles for KPP diffusion at times $t = 0 - 12$ hours. The KPP diffusion profile is calculated with $\theta = 1.0$, $u_{10} = 6.65$ m s^{-1}, and z_0 according to Equation 12.

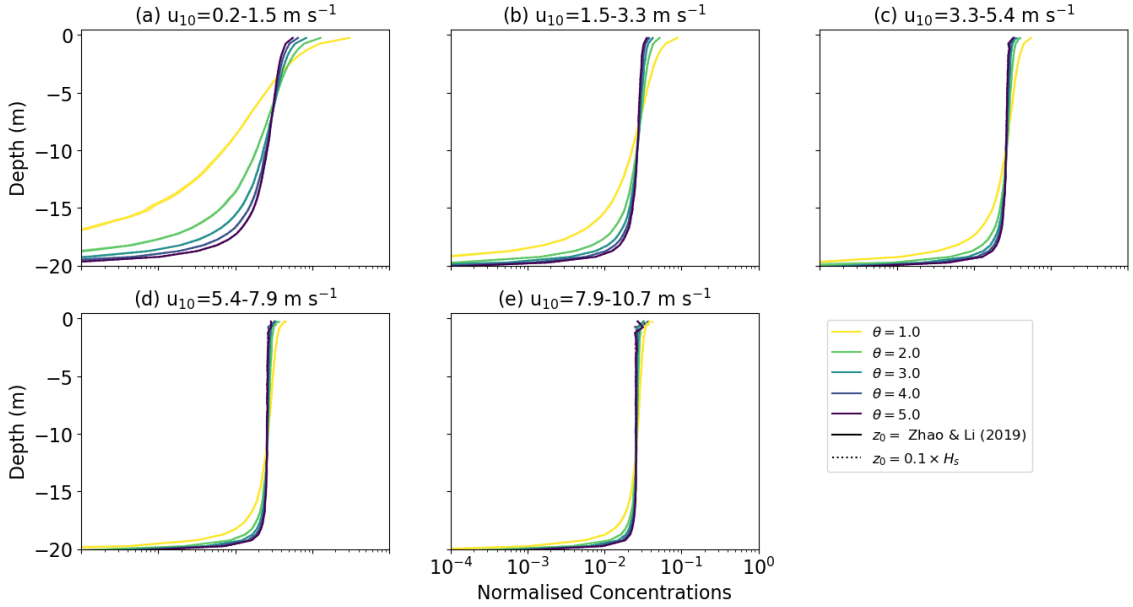

Figure D1. Vertical concentrations of buoyant particles for KPP diffusion under varying wind conditions with $w_r = 0.0003$ m s^{-1}. The KPP diffusion profile is calculated either with z_0 according to Equation 12 or $z_0 = 0.1 \times H_s$, and for $\theta \in [1.0, 2.0, 3.0, 4.0, 5.0]$. The grey markers indicate field measurements, with darker shades indicating more measurements, while the binned field measurement average and standard deviation are shown by the black markers. Shading around the profiles indicates the profile's standard deviation at each depth level.

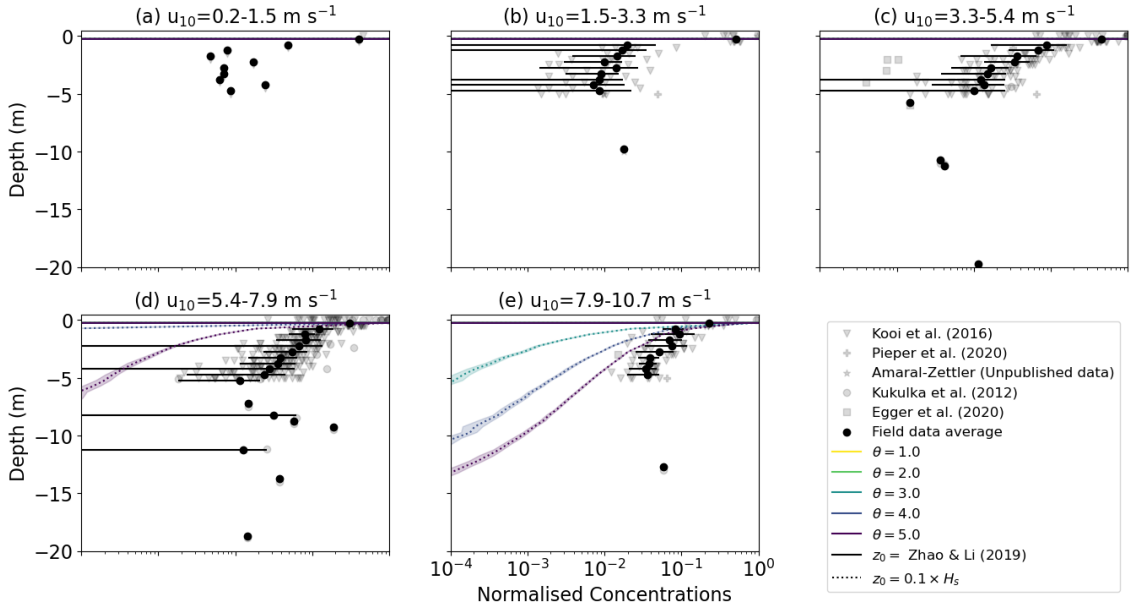

Figure D2. Vertical concentrations of buoyant particles for KPP diffusion under varying wind conditions with $w_r = 0.03$ m s^{-1}. The KPP diffusion profile is calculated either with z_0 according to Equation 12 or $z_0 = 0.1 \times H_s$, and for $\theta \in [1.0, 2.0, 3.0, 4.0, 5.0]$. The grey markers indicate field measurements, with darker shades indicating more measurements, while the binned field measurement average and standard deviation are shown by the black markers. Shading around the profiles indicates the profile's standard deviation at each depth level.

Appendix A: w_r/w' ratios for various turbulence scenarios

Appendix B: Influence of z_0 on diffusion profiles

Appendix C: Time evolution of concentration profiles

Appendix D: Influence of θ

Appendix E: Influence of Δt

Appendix F: Influence of boundary conditions

Author contributions. Development of the parametrizations and the analysis was done by VO, with CL helping with improving the code performance. The manuscript was written by VO, with extensive input from CL and EvS. Everyone contributed to the study design and discussion of the analysis.

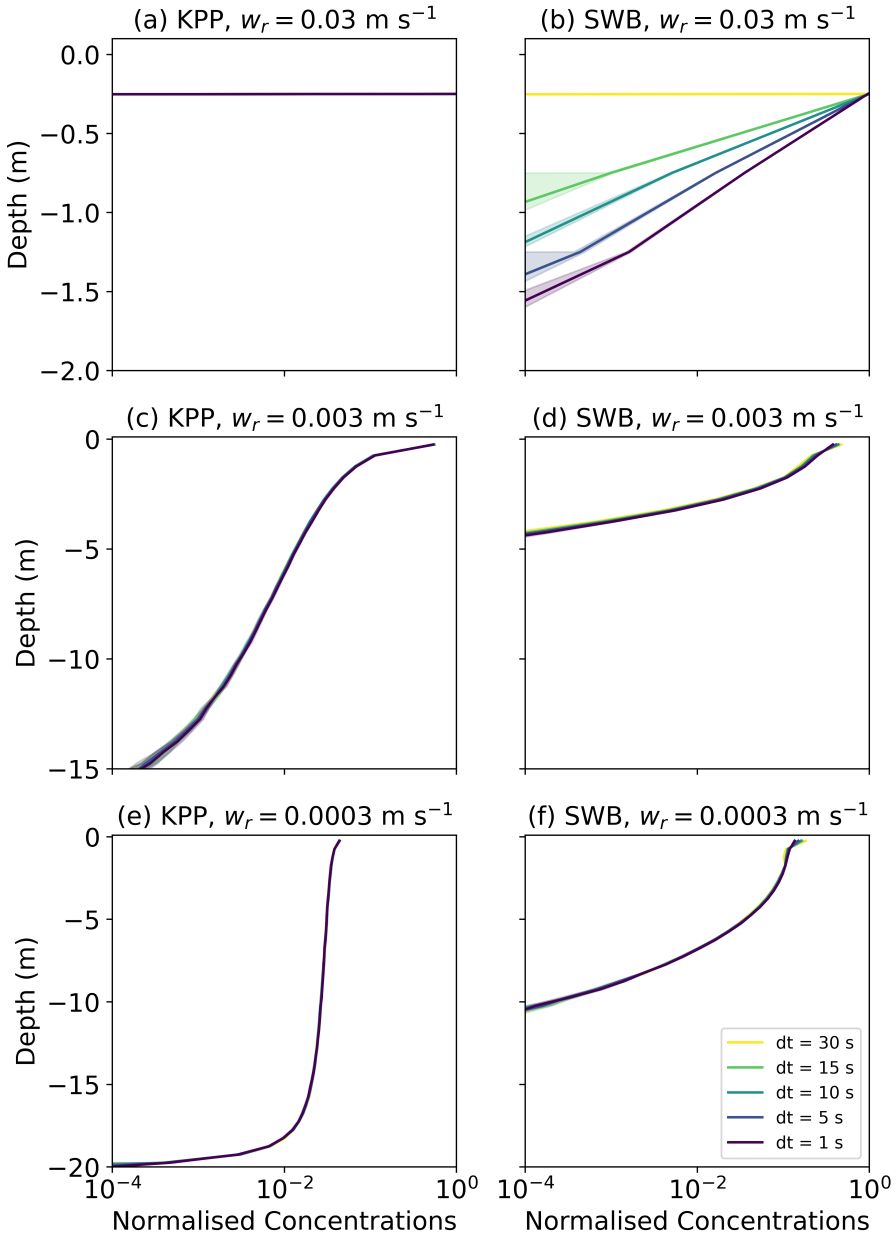

Figure E1. Vertical concentrations of buoyant particles for (a, c, e) KPP and (b, d, f) SWB diffusion using M-0 models with varying values for w_{rise} and $\Delta t \in [30, 15, 10, 5, 1]$ second(s). All profiles are for $u_{10} = 6.65$ m s^{-1}. Shading around the profiles indicates the profile's standard deviation at each depth level. The KPP profiles are computed with $\theta = 1.0$ and z_0 according to Equation 12.

Competing interests. The authors declare no competing interests.

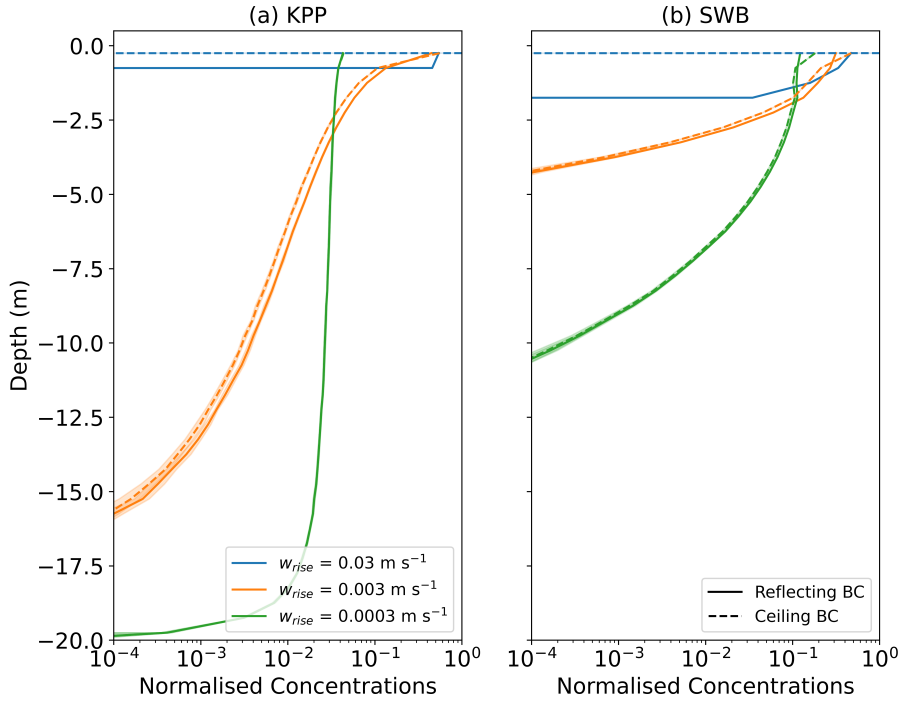

Figure F1. Vertical concentrations of buoyant particles for (a) KPP and (b) SWB diffusion using M-0 models for reflective and ceiling BC's. Shading around the profiles indicates the profile's standard deviation at each depth level. All profiles are for $u_{10} = 6.65$ m s^{-1}. The KPP profiles are computed with $\theta = 1.0$ and z_0 according to Equation 12.

Acknowledgements. VO and CL acknowledge support from the Swiss National Science Foundation (project PZ00P2_174124 Global interactions between microplastics and marine ecosystems). EvS was supported by the European Research Council (ERC) under the European Unions Horizon 2020 research and innovation programme (grant agreement No 715386). Calculations were performed on UBELIX (http://www.id.unibe.ch/hpc), the HPC cluster at the University of Bern. We would like to thank Dr. Tobias Kukulka, Dr. Catharina Pieper, Dr. Matthias Egger, Dr. Linda Amaral-Zettler and Dr. Erik Zettler for providing field measurements, Dr. Marie Poulain-Zarcos for providing data on vertical mixing, and Dr. Thomas Stocker and Daan Reijnders for fruitful discussions regarding the Markov-1 numerical schemes.

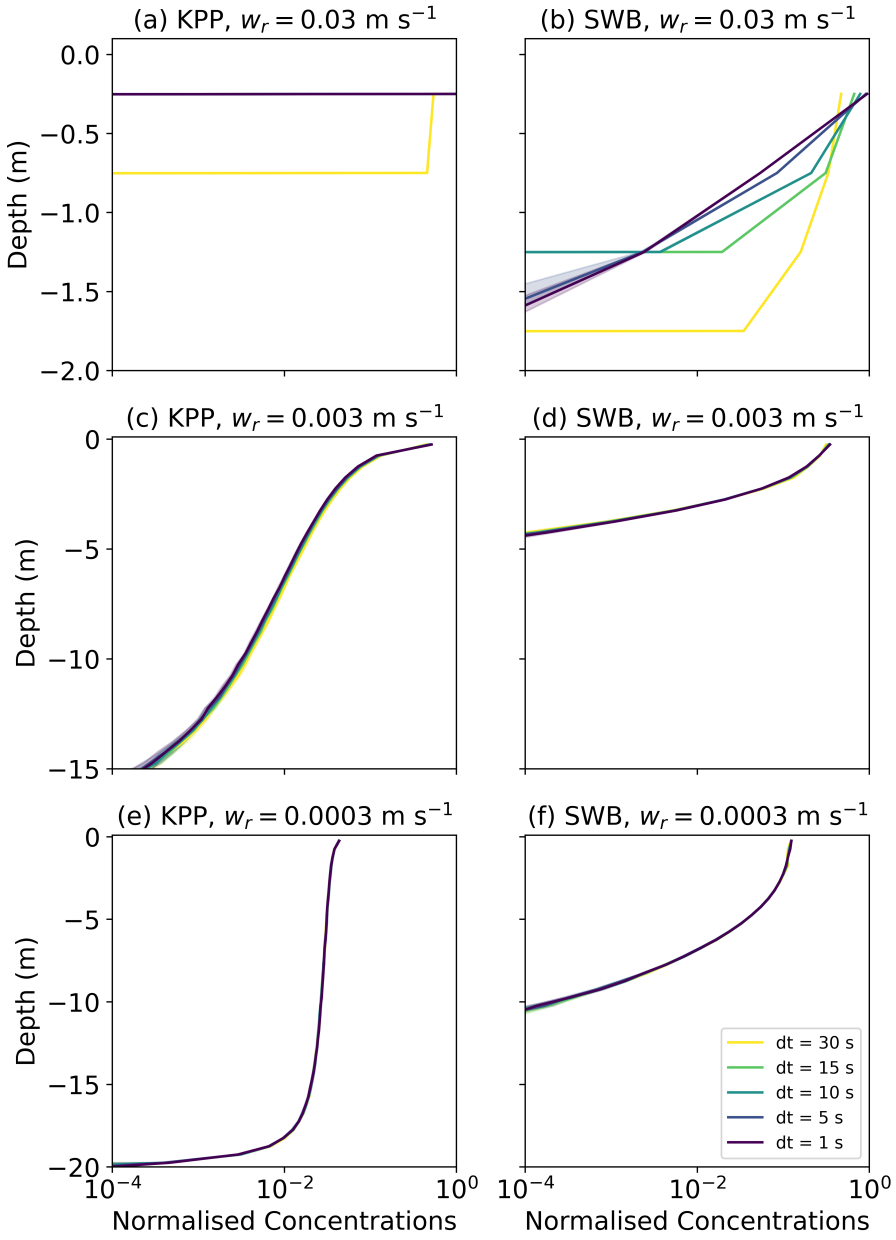

Figure F2. Vertical concentrations of buoyant particles for (a, c, e) KPP and (b, d, f) SWB diffusion using M-0 models with varying values for w_{rise} and $\Delta t \in [30, 15, 10, 5, 1]$ second(s) with a reflective BC. All profiles are for $u_{10} = 6.65$ m s^{-1}. Shading around the profiles indicates the profile's standard deviation at each depth level. The KPP profiles are computed with $\theta = 1.0$ and z_0 according to Equation 12.

References

Berloff, P. S. and McWilliams, J. C.: Material transport in oceanic gyres. Part III: Randomized stochastic models, Journal of physical oceanography, 33, 1416–1445, 2003.

Boufadel, M., Liu, R., Zhao, L., Lu, Y., Özgökmen, T., Nedwed, T., and Lee, K.: Transport of oil droplets in the upper ocean: impact of the eddy diffusivity, Journal of Geophysical Research: Oceans, 125, e2019JC015 727, 2020.

Brickman, D. and Smith, P.: Lagrangian stochastic modeling in coastal oceanography, Journal of atmospheric and oceanic technology, 19, 83–99, 2002.

Brignac, K. C., Jung, M. R., King, C., Royer, S.-J., Blickley, L., Lamson, M. R., Potemra, J. T., and Lynch, J. M.: Marine debris polymers on main Hawaiian Island beaches, sea surface, and seafloor, Environmental science & technology, 53, 12 218–12 226, 2019.

Brunner, K., Kukulka, T., Proskurowski, G., and Law, K. L.: Passive buoyant tracers in the ocean surface boundary layer: 2. Observations and simulations of microplastic marine debris, Journal of Geophysical Research: Oceans, 120, 7559–7573, 2015.

Chamecki, M., Chor, T., Yang, D., and Meneveau, C.: Material transport in the ocean mixed layer: recent developments enabled by large eddy simulations, Reviews of Geophysics, 57, 1338–1371, 2019.

Choy, C. A., Robison, B. H., Gagne, T. O., Erwin, B., Firl, E., Halden, R. U., Hamilton, J. A., Katija, K., Lisin, S. E., Rolsky, C., et al.: The vertical distribution and biological transport of marine microplastics across the epipelagic and mesopelagic water column, Scientific reports, 9, 1–9, 2019.

Craig, P. D. and Banner, M. L.: Modeling wave-enhanced turbulence in the ocean surface layer, Journal of Physical Oceanography, 24, 2546–2559, 1994.

de Boyer Montégut, C., Madec, G., Fischer, A. S., Lazar, A., and Iudicone, D.: Mixed layer depth over the global ocean: An examination of profile data and a profile-based climatology, Journal of Geophysical Research: Oceans, 109, 2004.

de Lavergne, C., Vic, C., Madec, G., Roquet, F., Waterhouse, A. F., Whalen, C., Cuypers, Y., Bouruet-Aubertot, P., Ferron, B., and Hibiya, T.: A parameterization of local and remote tidal mixing, Journal of Advances in Modeling Earth Systems, 12, e2020MS002 065, 2020.

Delandmeter, P. and Sebille, E. v.: The Parcels v2. 0 Lagrangian framework: new field interpolation schemes, Geoscientific Model Development, 12, 3571–3584, 2019.

Denman, K. and Gargett, A.: Time and space scales of vertical mixing and advection of phytoplankton in the upper ocean, Limnology and oceanography, 28, 801–815, 1983.

Egger, M., Sulu-Gambari, F., and Lebreton, L.: First evidence of plastic fallout from the North Pacific Garbage Patch, Scientific reports, 10, 1–10, 2020.

Enders, K., Lenz, R., Stedmon, C. A., and Nielsen, T. G.: Abundance, size and polymer composition of marine microplastics$\geq$ 10 μm in the Atlantic Ocean and their modelled vertical distribution, Marine pollution bulletin, 100, 70–81, 2015.

Fernando, H. J.: Turbulent mixing in stratified fluids, Annual review of fluid mechanics, 23, 455–493, 1991.

Fischer, R., Lobelle, D., Kooi, M., Koelmans, A., Onink, V., Laufkötter, C., Amaral-Zettler, L., Yool, A., and van Sebille, E.: Modeling submerged biofouled microplastics and their vertical trajectories, Biogeosciences Discussions, pp. 1–29, 2021.

Gaspar, P., Grégoris, Y., and Lefevre, J.-M.: A simple eddy kinetic energy model for simulations of the oceanic vertical mixing: Tests at station Papa and Long-Term Upper Ocean Study site, Journal of Geophysical Research: Oceans, 95, 16 179–16 193, 1990.

Gräwe, U., Deleersnijder, E., Shah, S. H. A. M., and Heemink, A. W.: Why the Euler scheme in particle tracking is not enough: the shallow-sea pycnocline test case, Ocean Dynamics, 62, 501–514, 2012.

Hopfinger, E. and Toly, J.-A.: Spatially decaying turbulence and its relation to mixing across density interfaces, Journal of fluid mechanics, 78, 155–175, 1976.

Kaiser, D., Kowalski, N., and Waniek, J. J.: Effects of biofouling on the sinking behavior of microplastics, Environmental Research Letters, 12, 124 003, 2017.

Kooi, M., Reisser, J., Slat, B., Ferrari, F., Schmid, M., Cunsolo, S., Brambini, R., Noble, K., Sirks, L.-A., Linders, T. E., Schoeneich-Argent, R. I., and Koelmans, A. A.: Data from 'The effect of particle properties on the depth profile of buoyant plastics in the ocean', https://doi.org/10.6084/m9.figshare.3427862.v1, 2016a.

Kooi, M., Reisser, J., Slat, B., Ferrari, F. F., Schmid, M. S., Cunsolo, S., Brambini, R., Noble, K., Sirks, L.-A., Linders, T. E., et al.: The effect of particle properties on the depth profile of buoyant plastics in the ocean, Scientific reports, 6, 1–10, 2016b.

Kukulka, T. and Brunner, K.: Passive buoyant tracers in the ocean surface boundary layer: 1. Influence of equilibrium wind-waves on vertical distributions, Journal of Geophysical Research: Oceans, 120, 3837–3858, 2015.

Kukulka, T. and Veron, F.: Lagrangian investigation of wave-driven turbulence in the ocean surface boundary layer, Journal of Physical Oceanography, 49, 409–429, 2019.

Kukulka, T., Proskurowski, G., Morét-Ferguson, S., Meyer, D., and Law, K.: The effect of wind mixing on the vertical distribution of buoyant plastic debris, Geophysical Research Letters, 39, 2012.

Landahl, M. T. and Christensen, E. M.: Turbulence and random processes in fluid mechanics, Cambridge University Press, 1998.

Large, W. and Pond, S.: Open ocean momentum flux measurements in moderate to strong winds, Journal of physical oceanography, 11, 324–336, 1981.

Large, W. G., McWilliams, J. C., and Doney, S. C.: Oceanic vertical mixing: A review and a model with a nonlocal boundary layer parameterization, Reviews of geophysics, 32, 363–403, 1994.

Law, K. L., More´t-Ferguson, S. E., Goodwin, D. S., Zettler, E. R., DeForce, E., Kukulka, T., and Proskurowski, G.: Distribution of surface plastic debris in the eastern Pacific Ocean from an 11-year data set, Environmental science & technology, 48, 4732–4738, 2014.

Lebreton, L., Slat, B., Ferrari, F., Sainte-Rose, B., Aitken, J., Marthouse, R., Hajbane, S., Cunsolo, S., Schwarz, A., Levivier, A., et al.: Evidence that the Great Pacific Garbage Patch is rapidly accumulating plastic, Scientific reports, 8, 1–15, 2018.

Liang, J.-H., McWilliams, J. C., Sullivan, P. P., and Baschek, B.: Large eddy simulation of the bubbly ocean: New insights on subsurface bubble distribution and bubble-mediated gas transfer, Journal of Geophysical Research: Oceans, 117, 2012.

Liubartseva, S., Coppini, G., Lecci, R., and Clementi, E.: Tracking plastics in the Mediterranean: 2D Lagrangian model, Marine pollution bulletin, 129, 151–162, 2018.

Lobelle, D., Kooi, M., Koelmans, A. A., Laufkötter, C., Jongedijk, C. E., Kehl, C., and van Sebille, E.: Global modeled sinking characteristics of biofouled microplastic, Journal of Geophysical Research: Oceans, 126, e2020JC017 098, 2021.

Maruyama, G.: Continuous Markov processes and stochastic equations, Rendiconti del Circolo Matematico di Palermo, 4, 48, 1955.

McWilliams, J. C. and Sullivan, P. P.: Vertical mixing by Langmuir circulations, Spill Science & Technology Bulletin, 6, 225–237, 2000.

Mofakham, A. A. and Ahmadi, G.: On random walk models for simulation of particle-laden turbulent flows, International Journal of Multiphase Flow, 122, 103 157, 2020.

Nordam, T., Kristiansen, R., Nepstad, R., and Röhrs, J.: Numerical analysis of boundary conditions in a Lagrangian particle model for vertical mixing, transport and surfacing of buoyant particles in the water column, Ocean Modelling, 136, 107–119, 2019.

Onink, V.: Model and analysis code for: "Empirical Lagrangian parametrization for wind-driven mixing of buoyant particulates at the ocean surface", https://doi.org/10.5281/ZENODO.4912693, https://zenodo.org/record/4912693, 2021.

Onink, V., Wichmann, D., Delandmeter, P., and van Sebille, E.: The role of Ekman currents, geostrophy, and stokes drift in the accumulation of floating microplastic, Journal of Geophysical Research: Oceans, 124, 1474–1490, 2019.

Onink, V., Jongedijk, C. E., Hoffman, M. J., van Sebille, E., and Laufkötter, C.: Global simulations of marine plastic transport show plastic trapping in coastal zones, Environmental Research Letters, 16, 064 053, 2021.

Paris, C. B., Atema, J., Irisson, J.-O., Kingsford, M., Gerlach, G., and Guigand, C. M.: Reef odor: a wake up call for navigation in reef fish larvae, PloS one, 8, e72 808, 2013.

Pieper, C., Martins, A., Zettler, E., Loureiro, C. M., Onink, V., Heikkilä, A., Epinoux, A., Edson, E., Donnarumma, V., de Vogel, F., et al.: INTO THE MED: Searching for Microplastics from Space to Deep-Sea, in: International Conference on Microplastic Pollution in the Mediterranean Sea, pp. 129–138, Springer, 2019.

Poulain, M.: Etude de la distribution verticale de particules plastiques dans l'océan : caractérisation, modélisation et comparaison avec des observations, Ph.D. thesis, Institut National Polytechnique de Toulouse, 6 allée Emile Monso - BP 34038 31029 Toulouse, 2020.

Poulain, M., Mercier, M. J., Brach, L., Martignac, M., Routaboul, C., Perez, E., Desjean, M. C., and Ter Halle, A.: Small microplastics as a main contributor to plastic mass balance in the North Atlantic Subtropical Gyre, Environmental science & technology, 53, 1157–1164, 2018.

Riisgård, H. U. and Larsen, P. S.: Viscosity of seawater controls beat frequency of water-pumping cilia and filtration rate of mussels Mytilus edulis, Marine Ecology Progress Series, 343, 141–150, 2007.

Ross, O. N. and Sharples, J.: Recipe for 1-D Lagrangian particle tracking models in space-varying diffusivity, Limnology and Oceanography: Methods, 2, 289–302, 2004.

Samaras, A. G., De Dominicis, M., Archetti, R., Lamberti, A., and Pinardi, N.: Towards improving the representation of beaching in oil spill models: A case study, Marine pollution bulletin, 88, 91–101, 2014.

Taylor, J. R.: Accumulation and subduction of buoyant material at submesoscale fronts, Journal of Physical Oceanography, 48, 1233–1241, 2018.

Thompson, S. and Turner, J.: Mixing across an interface due to turbulence generated by an oscillating grid, Journal of Fluid Mechanics, 67, 349–368, 1975.

Van Sebille, E., Griffies, S. M., Abernathey, R., Adams, T. P., Berloff, P., Biastoch, A., Blanke, B., Chassignet, E. P., Cheng, Y., Cotter, C. J., et al.: Lagrangian ocean analysis: Fundamentals and practices, Ocean Modelling, 121, 49–75, 2018.

Van Sebille, E., Aliani, S., Law, K. L., Maximenko, N., Alsina, J. M., Bagaev, A., Bergmann, M., Chapron, B., Chubarenko, I., Cózar, A., et al.: The physical oceanography of the transport of floating marine debris, Environmental Research Letters, 15, 023 003, 2020.

Waterhouse, A. F., MacKinnon, J. A., Nash, J. D., Alford, M. H., Kunze, E., Simmons, H. L., Polzin, K. L., St. Laurent, L. C., Sun, O. M., Pinkel, R., et al.: Global patterns of diapycnal mixing from measurements of the turbulent dissipation rate, Journal of Physical Oceanography, 44, 1854–1872, 2014.

Wichmann, D., Delandmeter, P., and van Sebille, E.: Influence of near-surface currents on the global dispersal of marine microplastic, Journal of Geophysical Research: Oceans, 124, 6086–6096, 2019.

Yang, D., Chamecki, M., and Meneveau, C.: Inhibition of oil plume dilution in Langmuir ocean circulation, Geophysical Research Letters, 41, 1632–1638, 2014.

Zhao, D. and Li, M.: Dependence of wind stress across an air–sea interface on wave states, Journal of Oceanography, 75, 207–223, 2019.